
Masters Theses

Student Theses and Dissertations

Spring 2017

Design and modeling of an aluminum smelting process to analyze aluminum smelter and identify the alternative uses of nuclear power small modular reactor

Rajesh Ramkrushna Patharabe

Follow this and additional works at: https://scholarsmine.mst.edu/masters_theses



Part of the [Chemical Engineering Commons](#)

Department:

Recommended Citation

Patharabe, Rajesh Ramkrushna, "Design and modeling of an aluminum smelting process to analyze aluminum smelter and identify the alternative uses of nuclear power small modular reactor" (2017). *Masters Theses*. 7860.

https://scholarsmine.mst.edu/masters_theses/7860

This thesis is brought to you by Scholars' Mine, a service of the Missouri S&T Library and Learning Resources. This work is protected by U. S. Copyright Law. Unauthorized use including reproduction for redistribution requires the permission of the copyright holder. For more information, please contact scholarsmine@mst.edu.

**DESIGN AND MODELING OF AN ALUMINUM SMELTING PROCESS TO
ANALYZE ALUMINUM SMELTER AND IDENTIFY THE ALTERNATIVE
USES OF NUCLEAR POWER SMALL MODULAR REACTOR**

by

RAJESH RAMKRUSHNA PATHARABE

A THESIS

Presented to the Faculty of the Graduate School of the

MISSOURI UNIVERSITY OF SCIENCE AND TECHNOLOGY

In Partial Fulfillment of the Requirements for the Degree

MASTER OF SCIENCE IN CHEMICAL ENGINEERING

2017

Approved by:

Dr. Joseph Smith, Advisor

Dr. Muthanna Al-Dahhan

Dr. Douglas Ludlow

© 2017
Rajesh Ramkrushna Patharabe
All Rights Reserved

PUBLICATION THESIS OPTION

This thesis consists of the following two articles, formatted in the style used by the Missouri University of Science and Technology:

Paper I: A Mimic Dynamic Simulation of a High Temperature Aluminum Smelting process to analyze Aluminum Smelter and to identify the Alternative Uses of Nuclear Power Small Modular Reactor, Pages 2-30 are intended for submission to INTERNATIONAL JOURNAL OF METALCASTING, American Foundry Journal.

Paper II: High Temperature Steam/CO₂ Co-electrolysis for the Utilization of Carbon Dioxide from Aluminum Smelting process for the production of Synthetic Gas, Pages 31-66 are intended for submission to INTERNATIONAL JOURNAL OF METALCASTING, American Foundry Journal.

ABSTRACT

This thesis focuses on design and analysis of an Aluminum Smelting process using computer simulation which performs a dynamic state computation. The objective is to develop a Dynamic Simulation Model of an Aluminum Smelter using Mimic Simulator to analyze the dynamic behavior of an Aluminum Smelter to evaluate strategies for alternative design or uses of Nuclear Power Small Modular Reactor to improve the efficiency of the process and to reduce the heat losses.

Increasing energy needs, decrease of the availability of cheap electricity and the need to reduce the greenhouse gases emissions are the biggest hurdles for running Aluminum smelters efficiently in industries. Developing a dynamic process model identifies different process parameters by performing a steady state and dynamic mass and heat balance. Mimic Simulation is an effective process modeling tool which can predict system ideal and non-ideal condition behavior and optimize the overall process.

The design and simulation approach for this process is similar to chemical processes with electrical heating and ionization effects of the chemical compounds are not considered. This work identifies the critical impact of Smelter temperature on Aluminum production and carbon dioxide emission and optimizes the electric heating require for the process. This system also employs a high temperature Steam/CO₂ Co-electrolysis unit for the utilization of carbon dioxide from Aluminum smelting for the production of synthetic gas using nuclear heat to support Missouri's Aluminum industry.

A Kinetic based dynamic model is developed to simulate a real system. Mimic predicted values which can be further validated with experimental results from real systems or industrial data.

ACKNOWLEDGEMENTS

I owe my deepest gratitude to my advisor, Dr. Joseph D. Smith, for accepting me into the Laufer Energy Research group. He has encouraged me to work on my own including spending a summer working at MYNAH Technologies. He provided me various opportunities to attend Small Modular Reactor Research and Education Consortium (SmrREC) meetings and Laufer Energy Symposium to showcase my research work. With him I have grown academically, professionally and personally. With the trust he placed in me to complete research work, I owe him a lot and I have no doubt in accepting that he has been the best part of my master of science study.

I would like to thank Dr. Muthanna Al-Dahhan and Dr. Douglas Ludlow for being a part of my thesis committee. I would like to thank Mr. Dave Sextro for allowing me to work at MYNAH Technologies during the summer on my research work. I would also wish to thank Mr. Rehman Fazeem and Sean Sullivan from MYNAH Technologies for their expert advices during various stages of my research work. I would like to thank Dr. Michael Devaney and Professor Gayla Neumeyer from University of Missouri Columbia for helping me with Literatures. I would like to thank Secretary Frieda Adams who has always responded and supported well during my research period.

Finally, I extend my personal thanks to my family for their continuous support and encouragement and all my lab mates at the Laufer Energy Research group: Prashant, Anand, Jeremy, Shyam, Vivek, Aso, Shruti, Teja, Manohar, Chen, Jia and Reza.

TABLE OF CONTENTS

	Page
PUBLICATION THESIS OPTION.....	iii
ABSTRACT.....	iv
ACKNOWLEDGEMENTS.....	v
LIST OF ILLUSTRATIONS.....	viii
LIST OF TABLES.....	xi
NOMENCLATURE	xii
 SECTION	
1. INTRODUCTION	1
 PAPER	
I. A MIMIC DYNAMIC SIMULATION OF A HIGH TEMPERATRUE ALUMINUM SMELTING PROCESS TO ANALYZE ALUMINUM SMELTER AND TO IDENTIFY THE ALTERNATIVE USES OF NUCLAR POWER SMALL MODULAR REACTOR.....	2
ABSTRACT.....	2
1. INTRODUCTION AND BACKGROUND	3
2. METHODOLOGY.....	6
3. MIMIC DYNAMIC SIMULATION	8
3.1 PRINCIPLES OF ALUMINUM SMELTING ELECTROLYSIS.....	8
3.2 KINETICS AND MECHANISM OF THE REACTION.....	11
3.3 MATERIAL AND ENERGY BALANCE.....	13
3.4 PROCESS MODEL AND CONTROLS.....	20

4. SIMULATION RESULTS.....	24
5. ECONOMIC ANALYSIS	27
6. CONCLUSION AND FUTURE WORK	28
REFERENCES	30
II. HIGH TEMPERATURE STEAM/CO ₂ CO-ELECTROLYSIS FOR THE UTILIZATION OF CARBON DIOXIDE FROM ALUMINUM SMELTING PROCESS FOR THE PRODUCTION OF SYNTHETIC GAS.....	31
ABSTRACT.....	31
1. INTRODUCTION AND BACKGROUND	32
2. METHODOLOGY	35
3. MIMIC DYNAMIC SIMULATION	38
3.1 PRINCIPLES OF HIGH TEMPERATURE CO-ELECTROLYSIS.....	38
3.2 KINETICS AND MECHANISM OF THE REACTION.....	44
3.3 MATERIAL AND ENERGY BALANCE.....	50
3.4 PROCESS MODEL AND CONTROLS.....	56
4. SIMULATION RESULTS	59
5. CONCLUSION AND FUTURE WORK	63
REFERENCES	65
SECTION	
2. CONCLUSIONS	67
APPENDIX.....	68
VITA.....	69

LIST OF ILLUSTRATIONS

Figure	Page
PAPER I	
1.1. Electrolytic Reduction of Alumina to Aluminum.....	3
1.2. U.S. Production of Primary Aluminum from 2000 to 2015.....	4
2.1. A Schematic Representation of an Aluminum Reduction Pot.....	6
3.1. Aluminum Smelter Reactor Sizing Configuration.....	15
3.2. Aluminum Smelter Reactor Initial Configuration at the start-up.....	16
3.3. Al Smelter Energy Balance Mimic Standard Model.....	17
3.4. Ideal Electrical Energy Required in KWh for Figure 3.3 Calc Block 1.....	18
3.5. Actual Electrical Energy Required in KWh for Figure 3.3 Calc Block 2.....	18
3.6. Specific Heat Loss Rate to the surrounding for Figure 3.3 Calc Block 3.....	19
3.7. Mimic Process Feed Model.....	20
3.8. Mimic Process Model.....	20
3.9. Aluminum Production Withdrawal Mimic Standard Model.....	21
3.10. Al Production Withdrawal programming for Figure 3.9 Calc Block 01.....	21
3.11. Al Production Withdrawal programming for Figure 3.9 Calc Block 02.....	22
3.12. Al Production Withdrawal programming for Figure 3.9 Calc Block 03.....	22
3.13. Mimic Al Smelter Process Controls.....	23
3.14. Mimic Process Control Standard Logic Models.....	23
4.1. Aluminum Smelter Operating Profile Simulation Results.....	24
4.2. Al ₂ O ₃ quantity fed for the simulation.....	25

4.3.	Al Smelter Final Product Composition.....	25
5.1.	A general PowerSim stock and flow base model for economic analysis of Primary Al Production in the US.....	27

PAPER II

1.1.	Solid Oxide Electrolysis Cell (SOEC) for Steam/CO ₂ Co-electrolysis	32
1.2.	CO ₂ -eq emissions for current electrolysis and thermochemical processes.....	33
1.3.	One Technology - Multiple modes of operation.....	34
2.1.	Working Mechanism of SOEC for Co-electrolysis of H ₂ O and CO ₂	35
2.2.	Energy Demand for High Temperature Co-electrolysis.....	36
3.1.	Operating cell voltage for Co-electrolysis by Idaho National Lab (INL).....	42
3.2.	Thermodynamics of Steam/CO ₂ Co-electrolysis for Syngas production.....	43
3.3.	Co-electrolysis Kinetics (Reaction Paths).....	45
3.4.	High-Temperature Steam/CO ₂ Electrolysis in SOEC using YSZ Electrolyte.....	47
3.5.	Syngas Reactor Sizing Configuration.....	52
3.6.	Syngas Reactor Initial Configuration at the start-up.....	52
3.7.	Syngas Energy Balance Mimic Standard Model.....	54
3.8.	Ideal Electrical Energy Required in KWh for Figure 3.7 Calc Block 1.....	54
3.9.	Actual Electrical Energy Required in KWh for Figure 3.7 Calc Block 2.....	55
3.10.	Specific Heat Loss Rate to the surrounding for Figure 3.7 Calc Block 3.....	55
3.11.	Mimic Process Feed Model.....	56
3.12.	Mimic Process Model.....	56
3.13.	Syngas reactor Production Withdrawal Mimic Standard Model.....	57
3.14.	Mimic Syngas Production Process Controls.....	57

3.15.	Mimic Process Control Standard Models.....	58
4.1.	Syngas reactor Production Operating Profile Simulation Results.....	59
4.2.	Syngas Reactor Final Product Composition.....	60
4.3.	CO ₂ and Steam quantity fed for the simulation.....	61

LIST OF TABLES

Table	Page
PAPER I	
3.1. Feed Inlet Stoichiometric Composition at the initial start-up	16
4.1. Theoretical and Actual (simulation) Results.....	26
PAPER II	
3.1. Tabulated values of ΔH^0 , ΔG^0 , V_0 and V_{tn} values.....	42
3.2. Feed Inlet Stoichiometric Composition at the initial start-up	53
4.1. Theoretical and Actual (simulation) Results.....	62

NOMENCLATURE

Symbol	Description
$^{\circ}\text{C}$	Degree celsius
kg	Kilogram
cm	Centimeter
kWh	Kilowatt hour
MWh	Megawatt hour
kA	Kiloampere
V	Volt
atm	Atmosphere
kJ	Kilojoule
kmols	Kilomoles
mole %	mole percentage
K	Kelvin
m^3	Cubic meter
sec^{-1}	Second inverse
kg/hr	Kilogram per hour
MMt	Million metric tons
A/cm^2	Ampere per square centimeter
kg/min	Kilogram per minute
ft^3	Cubic foot
kg/m^3	Kilogram per cubic meter

1. INTRODUCTION

This thesis is presented as two papers on Aluminum Smelting process and supportive Syngas production unit by High Temperature Steam/CO₂ Co-electrolysis. Detailed literature survey on both processes has been presented in each paper. In this introduction section, the focus will be on process design, modeling and simulation which form the basis for both papers.

Development and commercialization of any process requires extensive study, design, redesign and rebuilding. Each process has multiple steps and sometimes multiple routes to reach final product. Process Simulation is an important tool in process development and commercialization which helps right from screening new process to optimize existing process. A model transfers information from research to engineering to manufacturing and business team. The research goal is to design, simulate and develop the current and new system for two major chemical processes: Aluminum Smelting process and Syngas production process unit.

While modeling starts from a generic point, there are different Mimic advanced and standard unit models to account for additional mechanism to make the simulation better. Depending on what effects has to be studied, different approach can be considered for modeling but what is important is to target the unique aspect of any process. Key to this research is modeling a high temperature process and utilizing the byproduct to produce value-added product. Once a model is developed, how it can be used to further set design specification and perform a technical process optimization is another important part of the research which is presented in the following two papers.

PAPER

I. A MIMIC DYNAMIC SIMULATION OF A HIGH TEMPERATURE ALUMINUM SMELTING PROCESS TO ANALYZE ALUMINUM SMELTER AND TO IDENTIFY THE ALTERNATIVE USES OF NUCLEAR POWER SMALL MODULAR REACTOR

ABSTRACT

Increasing energy needs and decrease of the availability of cheap electricity are the biggest hurdles for running Aluminum Smelters efficiently in industries. Aluminum reduction cells are used to produce aluminum by electrolysis of aluminum oxide, a process known as the Hall-Heroult process. Due to energy intensive process and a limiting number of operational parameters that can be measured in an operating cell, the dynamics of the cell operation are really complicated to understand and improve.

In this work, the principles of Aluminum Smelting process are presented and a dynamic simulation model is developed to analyze and predict the dynamic behavior of an aluminum smelter and to evaluate strategies for alternative design or uses of a nuclear power SMR to explore intensive process heat energy requirement and to improve process efficiency. The model is based on an existing cell design which was being used by Noranda Inc. New Madrid, MO and some measurements data gathered from published articles by Noranda to do real-time simulation. The model is constructed in three parts; a material balance model, energy balance model and control model. The three parts are then combined into one overall model which may aid in the future improvements in control strategies and cell operation, as well as developing a predictive tool for the process itself.

1. INTRODUCTION AND BACKGROUND

Alumina is insoluble in all ordinary chemical reagents at room temperature and has a high melting point (above 2000 °C). These properties make conventional chemical processes used for reducing oxides difficult and impractical for conversion of alumina into aluminum. The commercial primary aluminum is produced by the electrochemical reduction of alumina. This process, commonly referred to as the Hall- Heroult process, is the primary method for aluminum production. The Hall-Heroult process takes place in an electrolytic cell or pot. In Figure 1.1, the cell consists of two electrodes (an anode and a cathode) and contains a molten bath of Sodium Aluminum Fluoride (Na_3AlF_6), known as Cryolite, which serves as an electrolyte and solvent for alumina. An electric current is passed through the bath, which reduces the alumina to form liquid aluminum and oxygen gas. The oxygen gas reacts with the carbon anode to form carbon dioxide. Molten aluminum collects at the cathode in the bottom of the cell and is removed by siphon.

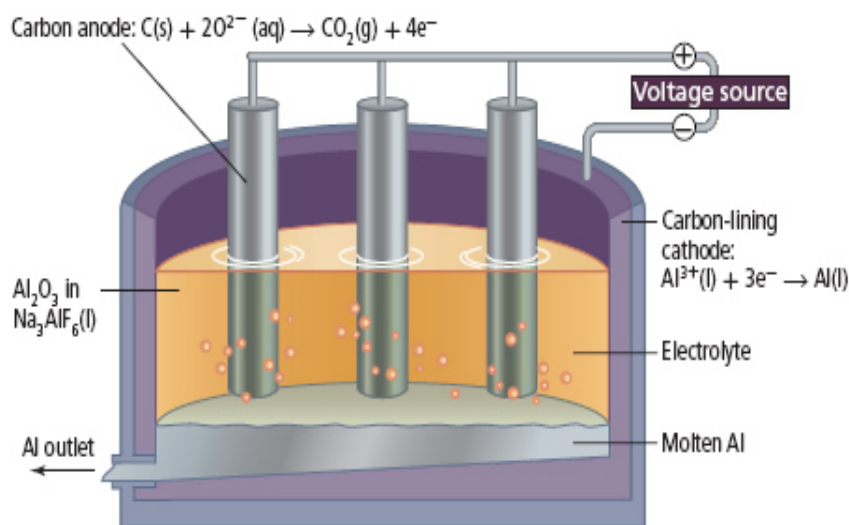


Figure 1.1. Electrolytic Reduction of Alumina to Aluminum [4]

The capacity and growth of Aluminum production in the US has decreased over the past 15 years. A significant process heat requirement is the biggest problem for running Aluminum smelters. In 2013, 5 companies operated 10 primary aluminum smelters; 3 smelters were closed for the entire year. Based on published market prices, the value of primary metal production was \$4.07 billion. The Figure 1.2 shows U. S. Production of Primary Aluminum from 2000 to 2015 (in Thousand Metric Dry Tons).

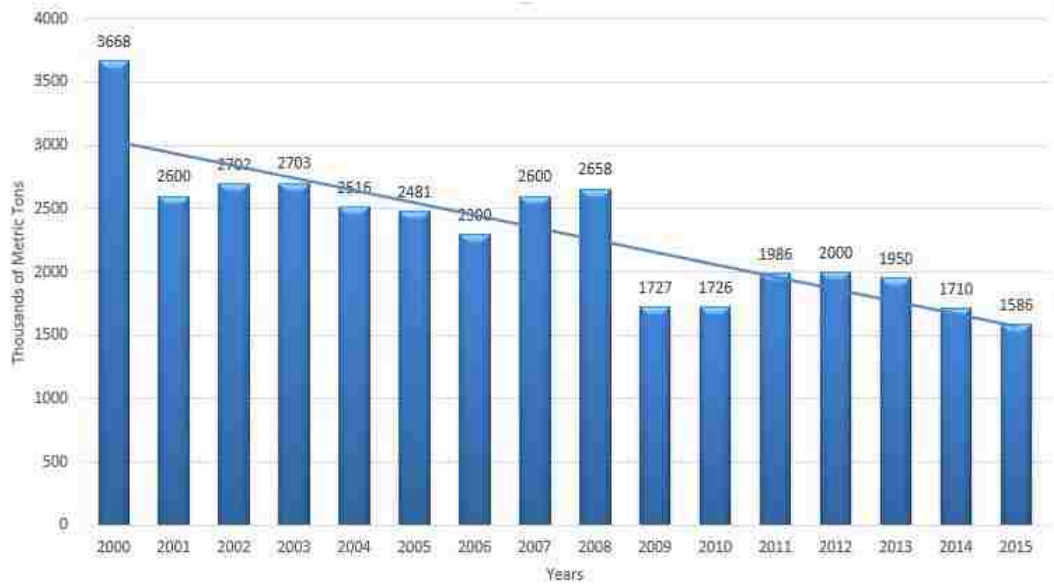


Figure 1.2. U. S. Production of Primary Aluminum from 2000 to 2015

In Aluminum industries, the process carbon consumption is in the range of 0.42 kg – 0.43 kg for each kg of aluminum production in most modern Hall-Heroult cells. Compared to the theoretical value of 0.33 kg of C/kg of Al, it is clear that electrochemical smelting technology is approaching a technological limit for the reduction of carbon consumption and the consequent emission of CO₂. The production of electricity used in the smelting process is another major, though indirect, source of CO₂ generation.

According to Environmental Protection Agency (EPA) and International Aluminum Institute (IAI), ‘the current average electricity requirement for smelting purposes is about 15.25 kWh per tons of aluminum’.

Motivation of this Research Study:

This research project is modeling the operations of primary aluminum smelting operation (with an electrical load of approximately 480 MW) and the 225 MWh Westinghouse Small Modular Reactor (WSMR). The Noranda site produced 260,000 metric tons of aluminum each year and was a major employer in the southeastern Missouri area.

In early 2016, Noranda Aluminum Inc. announced that it would stop operations of two of the three potlines due to technical operational issues, along with low commodity prices for aluminum and other business considerations. This action resulted in the layoff of 350 of its 900 employees, a huge economic impact in southeastern Missouri. In the intervening months, Noranda has ceased all operations, further reducing the site’s workforce and initiating Missouri Division of Workforce Development actions to support transition of workers to other jobs. In recent discussion with Noranda site personnel, the thought was expressed that if Noranda had access to energy costing 3 cents/kWh, Noranda’s New Madrid site would still be in business.

2. METHODOLOGY

The alumina reduction occurs in a vessel, which consists of several parts. There is an outer steel shell and some layers of thermally insulating bricks on the bottom to reduce heat losses from the bath. On top of these, there are some layers of refractory bricks which are very resistant to the high cell temperatures. The molten bath and aluminum are in a container made of carbon. The bottom part of the carbon container is called cathode. Under each cathode there is an iron bar, called collector bar, which transports the current out of the cell. A schematic representation of the aluminum reduction electrolysis pot is shown in Figure 2.1.

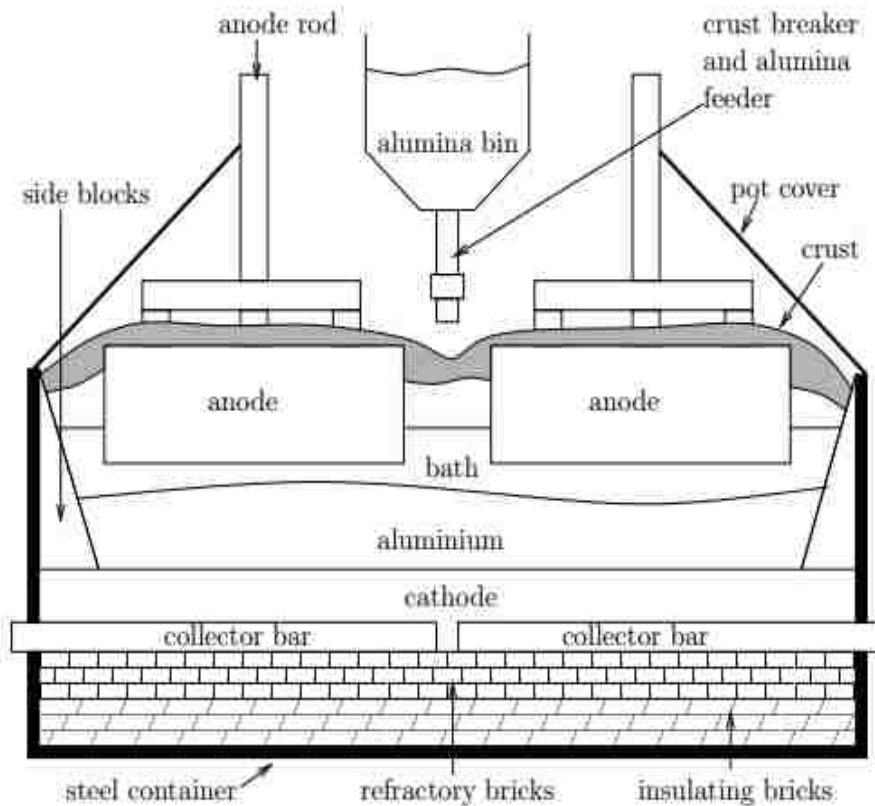


Figure 2.1. A Schematic Representation of an Aluminum Reduction Pot [6]

The bath and the aluminum are liquid due to the high temperature and they are separated because of different densities. The chemical reactions for the alumina reduction occur in the molten bath. The electrical current necessary for the electrolysis is transported to the bath through the carbon anodes which are partially immersed into the bath. Since the carbon of the anodes takes part in the chemical reaction, the anodes are slowly consumed and have to be replaced regularly. Between the anodes and the boundary of the cell, there is a protective layer, consisting of solidified bath and alumina, to prevent heat losses. It is called crust.

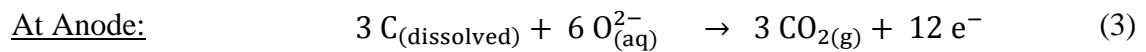
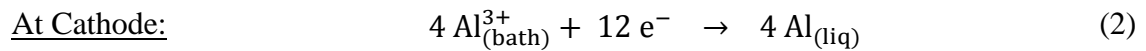
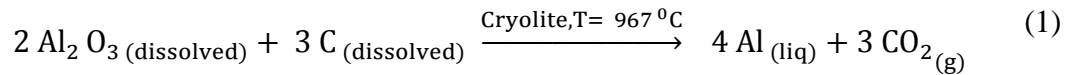
The CO₂ generated during the reaction escapes from the bath as gas bubbles. Since most of the surface of the bath is covered by the anodes, a bubble layer of CO₂ is built underneath the anodes in the bath. The aluminum formed by the reduction of alumina sinks to the bottom and increases the height of the liquids in the cell as the production goes on. The aluminum at the bottom has to be siphoned out regularly. During the electrolysis, the alumina dissolved in the bath is consumed and has to be restored periodically. Therefore, the cell is equipped with an alumina bin and a feeding system which delivers alumina to the electrolyte. In an aluminum production plants, there are usually hundreds of aluminum cells connected electrically in series.

In order to keep the bath at liquid state, the temperature of the bath has to be at about 967⁰C. This temperature is created by the electric resistance (Joule effect), mainly in the bath. To reach the right temperature with a current of about 325 kA, the height of the bath under the anode is only about 4 cm. The electric resistance is partly due to the gas bubble layers underneath the anodes, and depends also on the alumina concentration in the bath.

3. MIMIC DYNAMIC SIMULATION

3.1 PRINCIPLES OF ALUMINUM SMELTING ELECTROLYSIS

The Net electrochemical reaction of aluminum smelting inside the pot is



Modeling Principles & Approach:

- 1) Ionization effects of the chemical compounds and electrolytes are not considered
- 2) Aluminum oxide and Carbon are considered to be dissolved in the electrolyte at the initial ambient conditions
- 3) Dissociation rate of Al_2O_3 is kinetically dependent on activation energy and the concentration
- 4) Electrochemical deposition potential of Al_2O_3 electrolyzed with carbon anodes is considered to be known, $E_d = (-1.223/2) = -0.6115 \text{ V}$ at 967°C (from literature)
- 5) Dynamic Electrical heating is provided to the electrolytic reduction pot
- 6) Reaction temperature, pressure and volume variables are dynamic
- 7) Equilibrium Constant is varying with respect to temperature
- 8) Initial condition for Al Smelter are ambient (i.e. 1 atm pressure, and 25°C temp.)

The Heat of reaction is calculated by the equation

$$\Delta H^0_{(\text{reaction})} = \Delta H^0_{(\text{product})} - \Delta H^0_{(\text{reactant})} \quad (4)$$

$$= [(4 * \Delta H^0_{(\text{Al})}) + (3 * \Delta H^0_{(\text{CO}_2)})] - [(2 * \Delta H^0_{(\text{Al}_2\text{O}_3)}) + (3 * \Delta H^0_{(\text{C})})] \quad (5)$$

$$\begin{aligned}
&= [(4 * 0) + (3 * -394.838)] - [(2 * -1692.437) + (3 * 0)] \\
&= + 2,200.36 \text{ kJ/mol}
\end{aligned}$$

As ΔH of the reaction is positive, it means that reaction is endothermic and heat is absorbed by the system. The Gibbs free energy for the electrochemical reaction of alumina with carbon anodes in cryolite electrolyte is,

$$\Delta G_{(\text{cell})}^0 = - nFE_{(\text{cell})}^0 \quad (6)$$

Where, $E_{(\text{cell})}^0$ = Standard Electrode Potential at 25⁰C and 1 atm

n = Number of moles of electrons per mol of products

F = Faraday's constants = 96,485 Coulombs/mol

The larger the value of the standard reduction potentials (E^0), the easier it is for the element to be reduced (accept electrons). In other words, they are better oxidizing agents. Hence, the Gibb's free energy of formation at 967⁰C is

$$\Delta G_{(\text{cell})}^0 = \Delta G_{\text{f}(\text{product})}^0 - \Delta G_{\text{f}(\text{reactant})}^0 \quad (7)$$

$$= [(4 * \Delta G_{\text{f}(\text{Al})}^0) + (3 * \Delta G_{\text{f}(\text{CO}_2)}^0)] - [(2 * \Delta G_{\text{f}(\text{Al}_2\text{O}_3)}^0) + (3 * \Delta G_{\text{f}(\text{C})}^0)] \quad (8)$$

$$= [(4 * 0) + (3 * -396.098)] - [(2 * -1282.255) + (3 * 0)]$$

$$= + 1,376.216 \text{ kJ/mol}$$

The Gibb's free energies of formation of Aluminum and Carbon components are zero because they are pure elements and free energies of CO₂ and Al₂O₃ are taken from JANAF data table. As ΔG of the electrolytic reduction cell is positive, it means forward reaction is non-spontaneous. The electrochemical reaction of Al₂O₃ electrolyzed with Carbon Anode in cryolite is given by

$$E_{(\text{cell})}^0 = (-\Delta G_{(\text{cell})}^0/nF) \quad (9)$$

$$= (-1,376,216 \text{ J/mol}) / ((4*3)*96485 \text{ J/gm.eq.volt})$$

$$= - 1.189 \text{ V}$$

Where n = Number of electrons per mole of products i.e. $4 \text{ Al}_{(\text{liq})}^{3+} = (4*3) = 12$

F = Faraday's constant = 96,485 Coulombs/mol

The Aluminum, Carbon and CO_2 are nearly in the pure phase i.e. standard state, but Al_2O_3 is in standard phase only when it is at saturation. The Nernst Equation in the form of electro-chemical deposition potential (E_d), to calculate equilibrium constant (K_{eq}),

$$\Delta G = \Delta G^0 + RT * \ln K_{\text{eq}} \quad (10)$$

$$- nFE_d = - nFE^0 + RT * \ln K_{\text{eq}} \quad (11)$$

$$E_d = E^0 - \left(\frac{RT}{nF}\right) * \ln \frac{[\text{Oxd}]}{[\text{Red}]} = E^0 + \left(\frac{RT}{nF}\right) * \ln \frac{[\text{Red}]}{[\text{Oxd}]} \quad (12)$$

$$E_d = E^0 + \left(\frac{RT}{nF}\right) * \ln K_{\text{eq}} \quad (13)$$

$$- 0.6115 = - 1.189 + \left(\frac{8.314 * T}{12 * 96485}\right) * \ln K_{\text{eq}}$$

$$\ln K_{\text{eq}} = - 2367.445 * \left(\frac{1}{T}\right) \quad (14)$$

This is an equation of Equilibrium constant with respect to varying temperature. In this, ΔG^0 = Standard Gibb's free energy of formation of the cell and ΔG = Gibb's free energy of formation for Al_2O_3 electrolyzed with Carbon Anode. Comparing this with standard Mimic phase equilibrium constant equation,

$$\ln K_{\text{eq}} = A_1 + \left(\frac{A_2}{T}\right) + (A_3 * \ln(T)) + (A_4 * T) \quad (14)$$

It gives $A_1 = 0$, $A_2 = -2367.445$, $A_3 = 0$ and $A_4 = 0$.

3.2 KINETICS AND MECHANISM OF THE REACTION

In the literature, the overpotentials for the anodic reaction in the electrolysis of alumina dissolved in molten fluoride electrolytes have been measured by a steady-state technique using C, $\text{CO}_2+\text{CO}/\text{Al}_2\text{O}_3(\text{liq.})$ reference electrode. The overpotentials for the discharge of oxygen-containing anions in the systems $\text{Na}_3\text{AlF}_6+\text{CaF}_2+\text{Al}_2\text{O}_3$ and $(\text{Na}_3\text{AlF}_6+\text{Li})-(\text{AlF}_6+\text{Al}_2\text{O}_3)$ are reported as a function of current density, temperature and solvent composition. The Heat of activation evaluated from the temperature dependence is 13 ± 4 kcal/mole, which is in excellent agreement with the value determined by potentiostatic means. A theoretical kinetic analysis of possible anodic reactions leading to the evolution of CO_2 is presented. In each possible route, it appears that the rate-determining step is a two-electron transfer reaction in which oxide ions or oxygen-containing anions are discharged.

$$\begin{aligned} \text{The heat of activation or activation energy, } E_{(\text{act})} &= 13 \pm 4 \text{ kcal/mol} \\ &= 54.4 \pm 16.7 \text{ kJ/mol} \\ &= 54,400 \pm 16,700 \text{ kJ/kmol} \end{aligned}$$

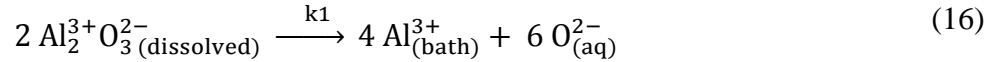
In this experimental study, anodic overpotentials for the electrolytic decomposition of alumina at a carbonaceous anode were determined with several partial pressures of CO_2 in Cryolite solvents represented by $3\text{Na}_3\text{AlF}_6+\text{CaF}_2$, $2\text{Na}_3\text{AlF}_6$, and $\text{Na}_3\text{AlF}_6+\text{Li}_3\text{AlF}_6$. The concentration of alumina was 17.1 mole % which is (approx. = $2/(2+3+4+3) = 16.7$ mole %) in all of these electrolytes. The measurements are carried out in the temperature range of 960°C to 1030°C .

There are several possible anions resulting from the salvation of alumina e.g. $\text{Al}_2^3+\text{O}_3^{2-}$, AlO_2^- , $\text{Al}_2\text{O}_2\text{F}_4^{2-}$, AlOF_2^- , AlOF_3^- etc., may be represented by the general

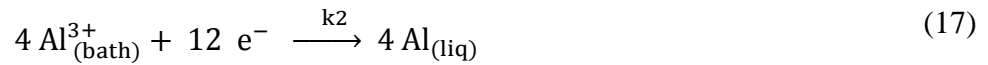
anionic formula, $Al_xO_yAl_z^{3x-2y-z}$. The following mechanisms would equally well apply to these anions. This case is considering Aluminum oxide, $Al_2^3+O_3^{2-}$.

The steps for the electrolysis of Aluminum oxide $Al_2^3+O_3^{2-}$ to Aluminum are

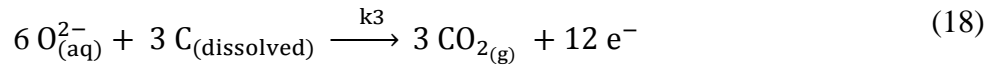
Step I) Dissociation of dissolved Aluminum Oxide



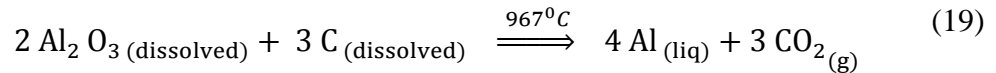
Step II) Cathodic reaction of Aluminum ions



Step III) Anodic reaction of Carbon and Oxygen ions



Step IV) Net reaction for the formation of Aluminum



Reaction IV is a rate determining step.

The net reaction rate, $r = r_f - r_b$ (20)

The expression for forward rate r_f of the overall reaction is

$$r_f = \left(k_{0f} * e^{\left(\frac{-E_{actf}}{RT} \right)} \right) * (\prod C_i^{a_f}) \quad (21)$$

$$r_f = \left(k_f * e^{\left(\frac{-E_{actf}}{RT} \right)} \right) * (C_{Al_2O_3(\text{dissolved})}^2 * C_{C(\text{dissolved})}^3) \quad (22)$$

The expression for backward rate r_b of the overall reaction is

$$r_b = \frac{k_b}{K_{eq}} * (\prod C_i^{a_b}) \quad (23)$$

$$r_b = \frac{k_f}{K_{eq}} * (C_{Al(liq)}^4 * C_{CO_2(g)}^3) \quad (24)$$

Where,

$$K_{eq} = \frac{(C_{Al(liq)}^4 * C_{CO_2(g)}^3)}{(C_{Al_2O_3(dissolved)}^2 * C_{C(dissolved)}^3)} = \frac{k_f}{k_b} \quad (25)$$

E_{act_f} (E_{act_b}) = Activation energy of the forward (reverse) reaction, KJ/kmol

R = Universal gas constant, kJ/(kmol*K) = 8.314 kJ/(kmol*K)

k_f (k_b) = rate constants for the forward (reverse)

C_i = Concentration of “i” component, molar fraction or kmol/m³

a_{i_f} (a_{i_b}) = partial order of the i component in forward (reverse) direction

Π = multiplication operator

f = characterizes the forward reaction

b = characterizes the backward reaction

The Activation energy (E_{act_f}) = 54,400 kJ/kmol (from the literature) and

Pre-exponential factor or forward reaction rate constant (k_f) = 0.05 sec⁻¹ (assumed).

3.3 MATERIAL AND ENERGY BALANCE

Material Balance:

The Aluminum Smelter plant capacity at Noranda New Madrid, MO = 260,000 MT/yr.

Basis: 260,000 MT/yr of Al production

Average operating rate of plant = 97%, where 3% is plant breakdown and shutdown

Hence, Primary Al operating capacity = $(0.97 * 260 * 10^6) \text{ kg/yr} = \left(\frac{0.97 * 260 * 10^6}{12 * 30 * 24} \right) \text{ kg/hr}$

$$= 29,190 \text{ kg/hr} = (31,435 \text{ kg} / 26.98 \text{ kg/kmol})$$

$$= 1082 \text{ kmol}$$

2 kmol of $\text{Al}_2\text{O}_3 = 4$ kmol of Al, therefore for 1082 kmol of Al,

$$\begin{aligned}\text{Al}_2\text{O}_3 \text{ required} &= (2/4) * 1082 = 541 \text{ kmol} \\ &= (541 \text{ kmol} * 101.96 \text{ kg/kmol}) = 55,160 \text{ kg/hr}\end{aligned}$$

$$\begin{aligned}\text{C required} &= (3/4) * 1082 = 811.5 \text{ kmol} \\ &= (811.5 \text{ kmol} * 12 \text{ kg/kmol}) = 9,738 \text{ kg/hr}\end{aligned}$$

$$\begin{aligned}\text{CO}_2 \text{ produced} &= (3/4) * 1082 = 811.5 \text{ kmol} \\ &= (811.5 \text{ kmol} * 44 \text{ kg/kmol}) = 35,706 \text{ kg/hr}\end{aligned}$$

In actual practice, feed Raw Materials will be excess, hence considering 5% excess RM

$$\text{Al}_2\text{O}_3 \text{ required} = (1.05 * 55160 \text{ kg/hr}) = 57,918 \text{ kg/hr}$$

$$\text{C required} = (1.05 * 9738 \text{ kg/hr}) = 10,225 \text{ kg/hr}$$

$$\text{Volume} = \frac{\text{Mass}}{\text{Density}}$$

$$V_{\text{C(dissolved)}} = \frac{10225 \text{ kg}}{1611 \text{ kg/m}^3} = 6.35 \text{ m}^3 \quad \text{Where, } \rho_{\text{C(liq)}} = 1611 \text{ kg/m}^3$$

$$V_{\text{Al}_2\text{O}_3(\text{dissolved})} = \frac{57918 \text{ kg}}{3053 \text{ kg/m}^3} = 18.97 \text{ m}^3 \quad \text{Where, } \rho_{\text{Al}_2\text{O}_3(\text{liq})} = 3053 \text{ kg/m}^3$$

$$\text{Hence, Total } V_{\text{CSTR(RM)}} = (6.35 + 18.97) = 25.32 \text{ m}^3$$

$$\text{Cryolite (Na}_3\text{AlF}_6\text{) Liquid Density} = 2 \text{ g/cm}^3 = 2 * 10^6 \text{ g/m}^3$$

Considering the Cryolite bath volume as same as Raw Material volume

$$\text{Hence, Cryolite quantity} = (2 * 10^6) \text{g/m}^3 * 25.32 \text{ m}^3 = 50,640 \text{ kg}$$

$$\text{Cryolite (Na}_3\text{AlF}_6\text{) Electrolyte Ratio} = \left(\frac{\text{NaF}}{\text{AlF}_3} \right) = \frac{3}{1} \quad (\text{Initial Concentration})$$

$$\text{Therefore, NaF quantity required} = \frac{3}{4} * 50,640 \text{ kg} = 37,980 \text{ kg, where Total} = (3+1) = 4$$

$$\text{AlF}_3 \text{ quantity required} = (50640 - 37980) = 12,660 \text{ kg}$$

$$\text{Total Liquid Volume of CSTR } V_{\text{CSTR(liq)}} = (V_{\text{Al}_2\text{O}_3(\text{dissolved})} + V_{\text{C(dissolved)}} + V_{\text{Na}_3\text{AlF}_6})$$

$$= (18.97 + 6.35 + 25.32) \text{ m}^3 = 50.64 \text{ m}^3$$

Considering 50% excess volume, Actual $V_{\text{CSTR}(\text{Total})} = (1.50 * 50.64) = 75.96 \text{ m}^3$

Reactor Sizing Configuration:

As vessel operating pressure $0 < P < 17$ bars, recommended $L/D = 3.5$. Now, for calculating the vessel sizing, the vessel diameter is given by

$$D = \left(\frac{V_{(T)}}{\left(\frac{1}{4}\right) * \pi * \left(\frac{L}{D}\right)} \right)^{1/3} \quad (26)$$

Reactor Diameter $D = 3.023 \text{ m}$, Reactor radius $r = 1.511 \text{ m}$

Reactor Length $L = \left(D * \frac{D}{L}\right) = (3.023 * 3.5) = 10.581 \text{ m}$

Initial Boundary Conditions: Pressure = 1.01325 atm, Temperature = 25⁰C

Boot Volume (Heavy Liquid (Al) Volume) = $\frac{m_{\text{Al}}}{\rho_{\text{Al}}} = \frac{29190 \text{ kg}}{2375 \text{ kg/m}^3} = 12.29 \text{ m}^3$, where

Figure 3.1 and 3.2 shows the Aluminum Smelter sizing and initial start-up configuration.

The screenshot shows the 'Reactor Configuration' window with the following settings:

- Reactor Type:** Vertical (selected), Horizontal
- Spherical Ends:** Top, Bottom
- Number of Inputs (1-8):** 6
- Number of Outputs (1-8):** 3
- Reactor Radius:** 1.511 m
- Reactor Height:** 10.58 m
- Reactor Minor Radius:** 0 m
- Initial Conditions:** Pressure - Temp (Calc Level) (selected), Pressure - Level (Calc Temp)
- Initial Temperature:** 25 °C
- Initial Sight Glass Level:** 0 %
- Initial Pressure:** 1.01325 atm
- Two Liquid Phases:** Two Liquid Phases (checked)
- Select Heavy Component(s):** Setup button
- Boot Volume:** 12.29 m³

Figure 3.1. Aluminum Smelter Reactor Sizing Configuration

Reactor Configuration

Units Settings 1 Settings 2 Agitator Elevations Heat Source Composition Reaction

Component Set
AL_PLANT [Change]

Activity Coefficients
 External []
 Constant

Fraction type
 Mole Fraction
 Mass Fraction

Solid	Component	Fraction	Activity
No	ALUMINUM_AL	0.000000	0.001000
No	CARBON_C	0.000000	0.001000
No	ALU_OXIDE_AL2O3	0.000000	0.001000
No	CARBON DIOXIDE	0.000000	200.000000
No	SOD_FLUORIDE_NAF	0.000000	0.001000
No	ALU_FLUORIDE_ALF3	0.000000	0.001000
No	NITROGEN	0.790000	200.000000
No	OXYGEN	0.210000	200.000000
No	CARBON MONOXIDE	0.000000	200.000000
Total:		1.000000	

[Zero] [Normalize]

Figure 3.2. Aluminum Smelter Reactor Initial Configuration at the start-up

The activities of components are calculated based on the component phases i.e. liquid or gas phase. Table 3.1 shows feed inlet stoichiometric composition at the start-up.

Table 3.1. Feed Inlet Stoichiometric Composition at the initial start-up

Components	MW (kg/kmol)	Feed Flow (kg/hr)	Feed Flow (kmol/hr)	Mass Frac. (wt %)	Mole Frac. (mol %)	Activity
Al	26.98	2.72E-04	1.01E-05	1.01E-05	4.19E-09	0.001
C	12	9,738	811.5	0.0843	0.3370	0.001
Al ₂ O ₃	101.96	55,160	541	0.4774	0.2247	0.001
CO ₂	44	2.61E-08	5.94E-10	5.9356E-10	2.47E-13	200
NaF	41.99	37,980	904.5	0.3287	0.3757	0.001
AlF ₃	83.98	12,660	150.75	0.1096	0.0626	0.001
N ₂	28.01	1.13E-03	4.03E-05	4.0289E-05	1.67E-08	200
O ₂	32	3.80E-04	1.19E-05	1.1873E-05	4.93E-09	200
CO	28.01	2.08E-08	7.41E-10	7.4090E-10	3.08E-13	200

Energy Balance:

The total energy associated with the primary aluminum production from bauxite ore was approximately 23.78 kWh/kg of aluminum in 2003. This consisted of

- 8.20 kWh/kg of aluminum for raw materials (Bayer process), and
- 15.58 kWh/kg of aluminum for electrolytic reduction (Hall-Heroult process).

The Aluminum Smelter energy calculation standard model shows the heat duty required to run the aluminum production electrolytic reduction cell in kWh as shown in Figure 3.3.

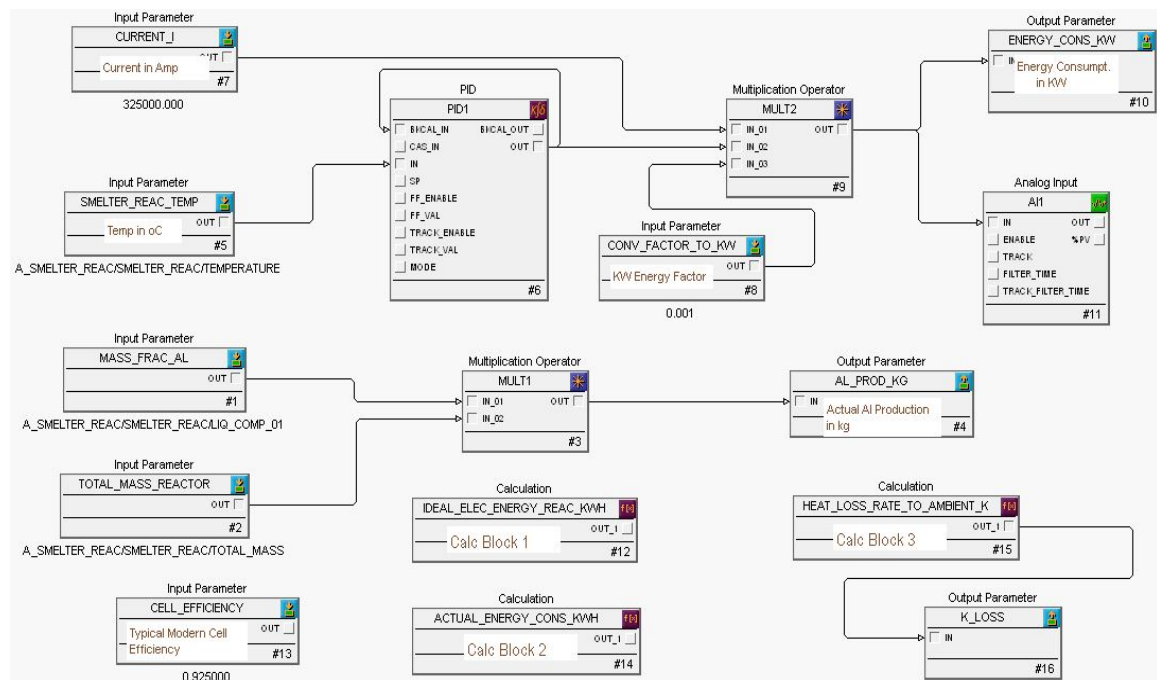
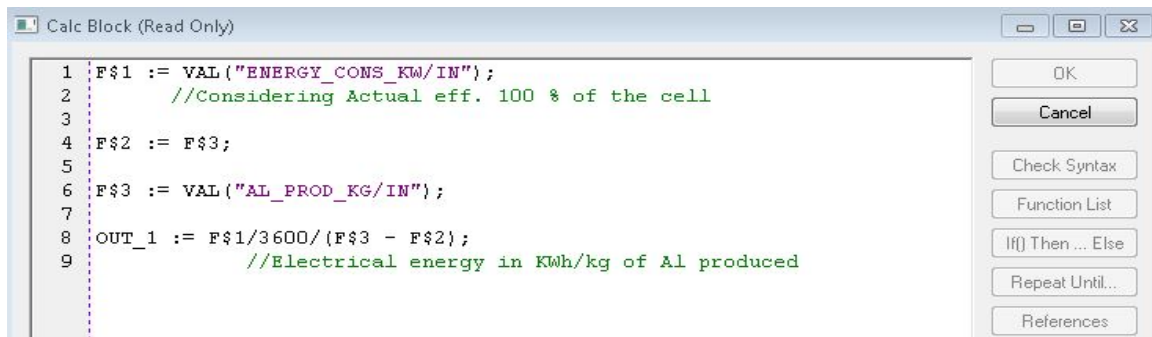


Figure 3.3. Al Smelter Energy Balance Mimic Standard Model

The electrochemical reaction potential of Al_2O_3 electrolyzed with carbon anodes in cryolite electrolyte is found to be 4 - 4.5 Volts considering 92.5% efficiency of the electrolytic cell and the actual electrical energy required for the electrolytic reduction cell is in the range of 14.5 – 16 kWh per kg of aluminum production in the simulation results.

The theoretical (ideal) electrical heat energy in kWh required per kg of Al produced to run the electrolytic cell at 100% efficiency found to be approximately 13-14 kWh and is calculated in Mimic simulator as shown in Figure 3.4.

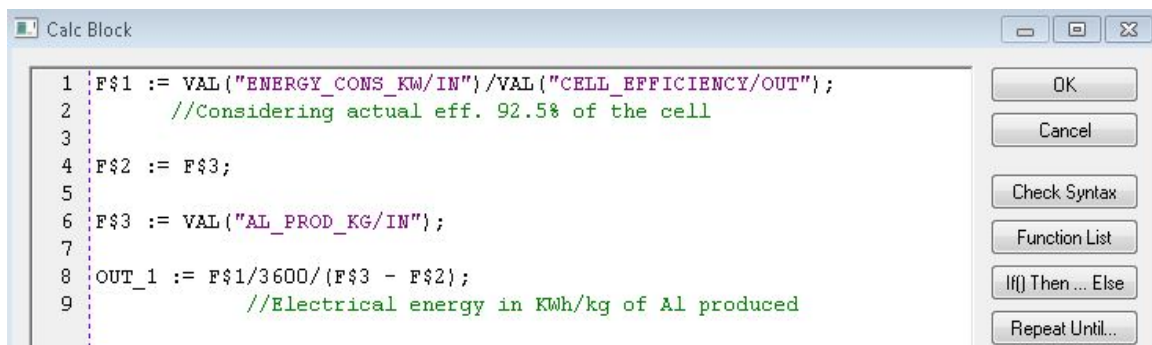


```

1 F$1 := VAL("ENERGY_CONS_KW/IN");
2     //Considering Actual eff. 100 % of the cell
3
4 F$2 := F$3;
5
6 F$3 := VAL("AL_PROD_KG/IN");
7
8 OUT_1 := F$1/3600/(F$3 - F$2);
9     //Electrical energy in KWh/kg of Al produced
  
```

Figure 3.4. Ideal Electrical Energy Required in KWh for Figure 3.3 Calc Block 1

The calculation for actual in-plant electrical heat energy in kWh required per kg of Al produced for the electrolytic cell at 92.5% efficiency is shown in Figure 3.5.



```

1 F$1 := VAL("ENERGY_CONS_KW/IN")/VAL("CELL_EFFICIENCY/OUT");
2     //Considering actual eff. 92.5% of the cell
3
4 F$2 := F$3;
5
6 F$3 := VAL("AL_PROD_KG/IN");
7
8 OUT_1 := F$1/3600/(F$3 - F$2);
9     //Electrical energy in KWh/kg of Al produced
  
```

Figure 3.5. Actual Electrical Energy Required in KWh for Figure 3.3 Calc Block 2

The heat energy tends to distribute itself evenly until a perfectly diffused uniform thermal field is achieved. Heat tends to flow from higher temperature zones by conduction, convection and radiation. The rate of heat flow by any of these forms is

determined by the temperature difference between the zones or area considered. The greater the temperature difference, the faster the rate of heat flow. The Specific Rate of Heat loss to Ambient is the rate of heat exchange to the environment, which is given by the equation

$$K_{\text{LOSS}} = \left(\frac{Q_{\text{LOSS}}}{M_{\text{S}_{\text{nom}}} * (T_{\text{S}_{\text{nom}}} - T_{\text{amb}})} \right) \quad (27)$$

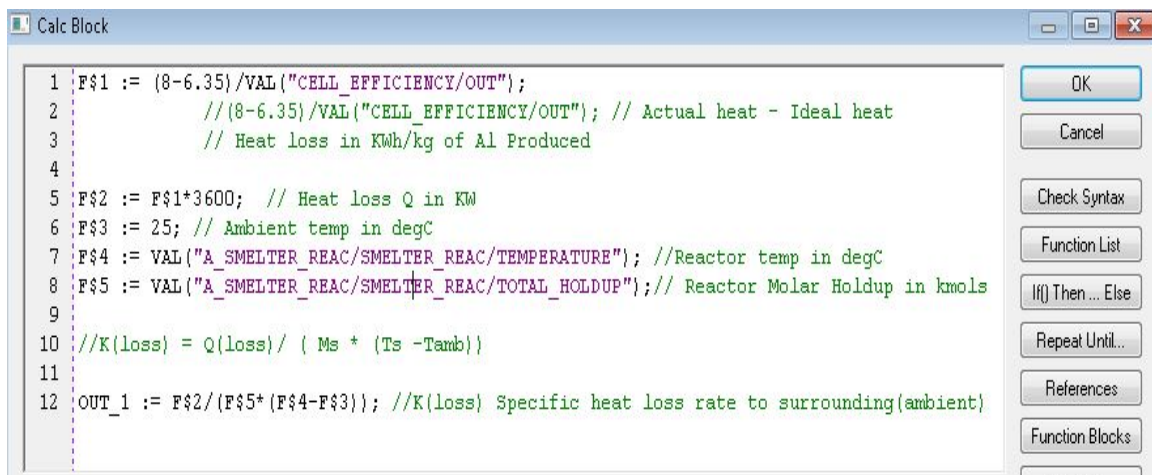
Where, Q_{LOSS} = Rate of heat exchange with the environment

$M_{\text{S}_{\text{nom}}}$ = Mass of material in the reactor, at the nominal state

$T_{\text{S}_{\text{nom}}}$ = Temperature of the material in the reactor, at the nominal state

T_{amb} = Temperature of the environment

The Actual electrical energy required to run the aluminum production electrolytic reaction is approximately 8 kWh. Here, the heat loss to the surrounding needs to be considered. Hence the Specific Rate of Heat loss (K_{LOSS}) of the electrolytic cell to ambient in $\text{kW} \cdot \text{C}^{-1} \cdot \text{kmol}^{-1}$ in Mimic Simulation is calculated as shown in Figure 3.6.



```

1 F$1 := (8-6.35)/VAL("CELL_EFFICIENCY/OUT");
2       //(8-6.35)/VAL("CELL_EFFICIENCY/OUT"); // Actual heat - Ideal heat
3       // Heat loss in KWh/kg of Al Produced
4
5 F$2 := F$1*3600; // Heat loss Q in KW
6 F$3 := 25; // Ambient temp in degC
7 F$4 := VAL("A_SMELTER_REAC/SMELTER_REAC/TEMPERATURE"); //Reactor temp in degC
8 F$5 := VAL("A_SMELTER_REAC/SMELTER_REAC/TOTAL_HOLDUP"); // Reactor Molar Holdup in kmols
9
10 //K(loss) = Q(loss) / ( Ms * (Ts -Tamb))
11
12 OUT_1 := F$2/(F$5*(F$4-F$3)); //K(loss) Specific heat loss rate to surrounding(ambient)

```

Figure 3.6. Specific Heat Loss Rate to the surrounding for Figure 3.3 Calc Block 3

3.4 PROCESS MODEL AND CONTROLS

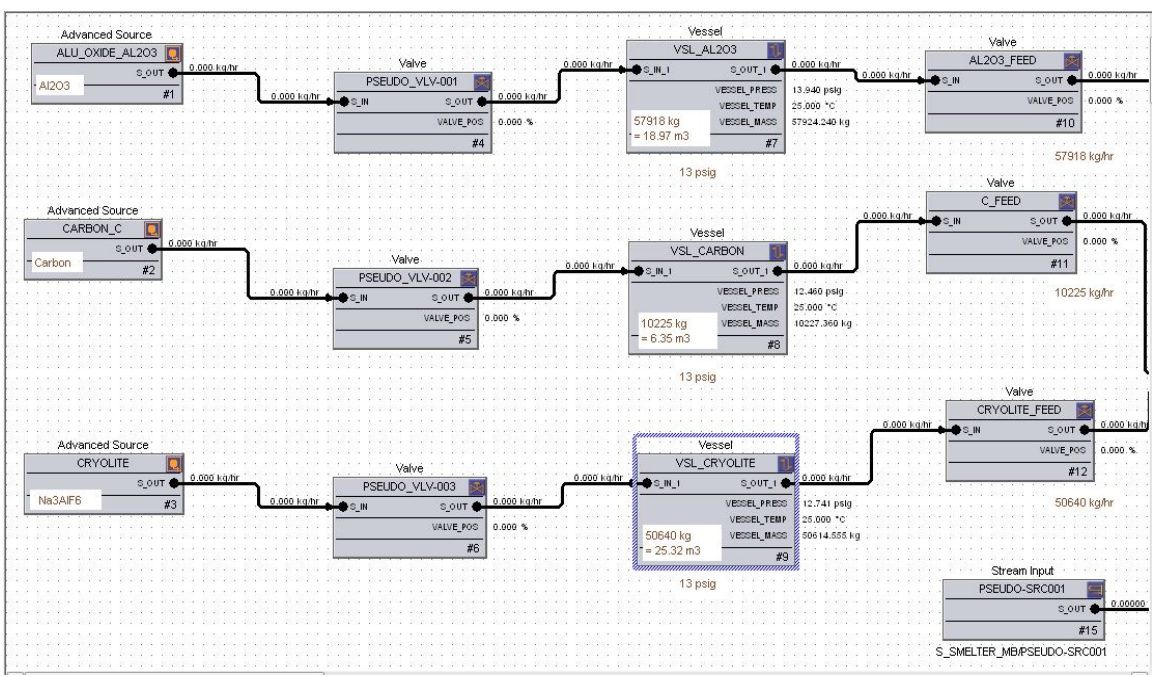


Figure 3.7. Mimic Process Feed Model

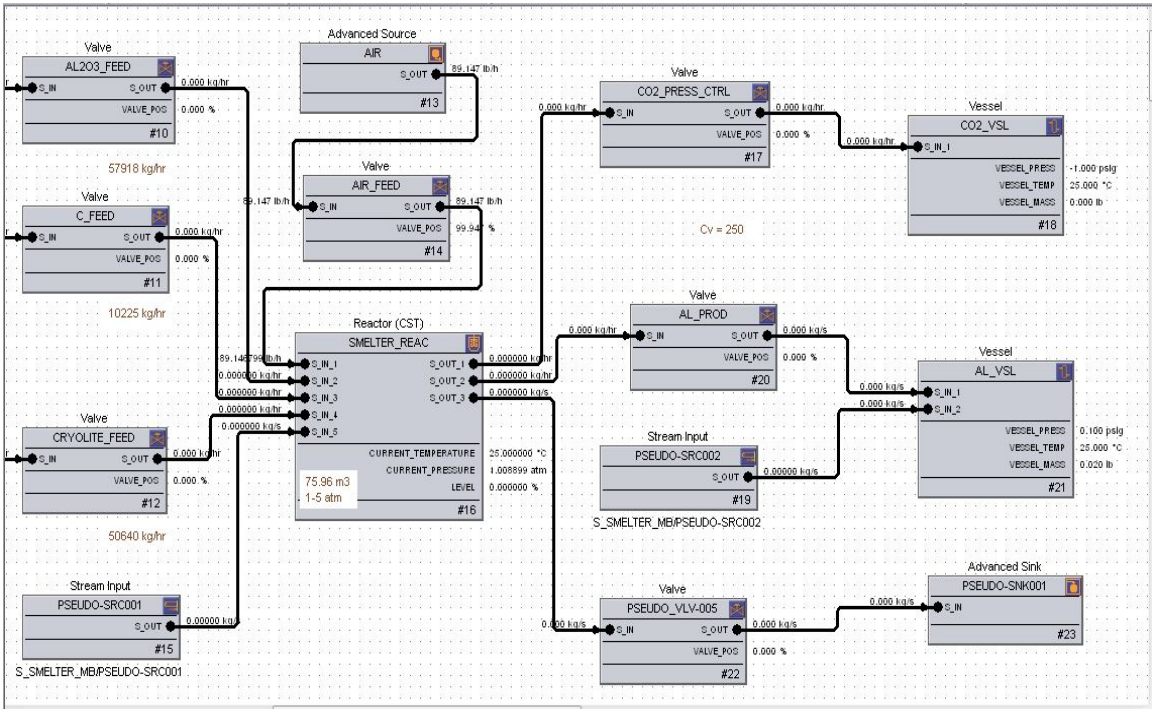


Figure 3.8. Mimic Process Model

Above Figure 3.7 and 3.8 shows Mimic Aluminum Smelting batch process model, with the aluminum metal deposited at the bottom of the pots and periodically siphoned off. Figure 3.9, 3.10, 3.11 and 3.12 shows the Mimic Al process production withdrawal model for taking off 33.33% of Al material each iteration from total Al production and returning 66.67% Al production with remaining component in the system back.

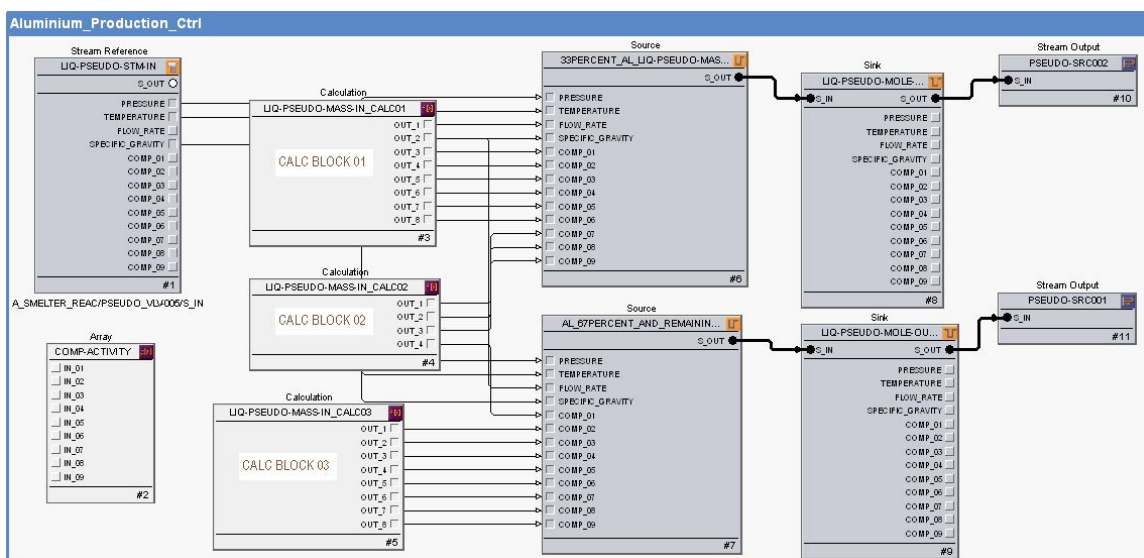


Figure 3.9. Aluminum Production Withdrawal Mimic Standard Model

```

1 // Total mass flow after manipulation
2
3 F$1 := VAL("LIQ-PSEUDO-STM-IN/FLOW_RATE"); //Total flow
4 F$2 := F$1 - F$1*(VAL("LIQ-PSEUDO-STM-IN/COMP_02")+VAL("LIQ-PSEUDO-STM-IN/COMP_03")+
5 VAL("LIQ-PSEUDO-STM-IN/COMP_04")+ VAL("LIQ-PSEUDO-STM-IN/COMP_05")+
6 VAL("LIQ-PSEUDO-STM-IN/COMP_06")+ VAL("LIQ-PSEUDO-STM-IN/COMP_07")+
7 VAL("LIQ-PSEUDO-STM-IN/COMP_08")+VAL("LIQ-PSEUDO-STM-IN/COMP_09"));
8 //Aluminium flow rate
9 OUT_1 := 0.3333*F$2;
10
11 OUT_2 := (F$1-F$2)+(0.6667*F$2); //Total flow rate except Al flow rate
12
13 //Component mass fractions after manipulation
14 OUT_3 := 1;//Al
15 OUT_4 := 0;//F$3*VAL("LIQ-PSEUDO-STM-IN/COMP_01");//C
16 OUT_5 := 0;//F$3*VAL("LIQ-PSEUDO-STM-IN/COMP_01");//Al2O3
17 OUT_6 := 0;//F$3*VAL("LIQ-PSEUDO-STM-IN/COMP_01");//CO2
18 OUT_7 := 0;//F$3*VAL("LIQ-PSEUDO-STM-IN/COMP_01");//NaF
19 OUT_8 := 0;//F$3*VAL("LIQ-PSEUDO-STM-IN/COMP_01");//AlF3

```

Figure 3.10. Al Production Withdrawal programming for Figure 3.9 Calc Block 01

```

2 // Total mass flow after manipulation
3
4 F$1 := VAL("LIQ-PSEUDO-STM-IN/FLOW_RATE"); //Total flow
5 F$2 := F$1 - F$1*(VAL("LIQ-PSEUDO-STM-IN/COMP_02")+VAL("LIQ-PSEUDO-STM-IN/COMP_03")+
6         VAL("LIQ-PSEUDO-STM-IN/COMP_04")+ VAL("LIQ-PSEUDO-STM-IN/COMP_05")+
7         VAL("LIQ-PSEUDO-STM-IN/COMP_06")+ VAL("LIQ-PSEUDO-STM-IN/COMP_07")+
8         VAL("LIQ-PSEUDO-STM-IN/COMP_08")+VAL("LIQ-PSEUDO-STM-IN/COMP_09"));
9         //Aluminium flow rate
10
11 //Component mass fractions after manipulation
12 OUT_1 := 0; //F$3*VAL("LIQ-PSEUDO-STM-IN/COMP_01")//N2
13 OUT_2 := 0; //F$3*VAL("LIQ-PSEUDO-STM-IN/COMP_01")//O2
14 OUT_3 := 0; //F$3*VAL("LIQ-PSEUDO-STM-IN/COMP_01")//CO
15 OUT_4 := ((F$1-F$2)+(0.6667*F$2))*VAL("LIQ-PSEUDO-STM-IN/COMP_01");
           //Mass fraction of Al returning back to CSTR

```

Figure 3.11. Al Production Withdrawal programming for Figure 3.9 Calc Block 02

```

1 // Total mass flow after manipulation
2
3 F$1 := VAL("LIQ-PSEUDO-STM-IN/FLOW_RATE"); //Total flow
4
5 //Component mass fractions after manipulation
6 OUT_1 := VAL("LIQ-PSEUDO-STM-IN/COMP_02")*F$1;
7 OUT_2 := VAL("LIQ-PSEUDO-STM-IN/COMP_03")*F$1;
8 OUT_3 := VAL("LIQ-PSEUDO-STM-IN/COMP_04")*F$1;
9 OUT_4 := VAL("LIQ-PSEUDO-STM-IN/COMP_05")*F$1;
10 OUT_5 := VAL("LIQ-PSEUDO-STM-IN/COMP_06")*F$1;
11 OUT_6 := VAL("LIQ-PSEUDO-STM-IN/COMP_07")*F$1;
12 OUT_7 := VAL("LIQ-PSEUDO-STM-IN/COMP_08")*F$1;
13 OUT_8 := VAL("LIQ-PSEUDO-STM-IN/COMP_09")*F$1;

```

Figure 3.12. Al Production Withdrawal programming for Figure 3.9 Calc Block 03

The controls for Aluminum production exemplifies a detail understanding of process variability, and how to diagnose abnormalities and its causes in aluminum production plants. It presents information in an easy to format mode, without formulae or technological complexity. Figure 3.13 shows the Mimic Aluminum process control view for the running the process operation and Figure 3.14 shows the Mimic Process Control standard models logics for controlling the feed, products and process streams flow, temperature and pressure etc.

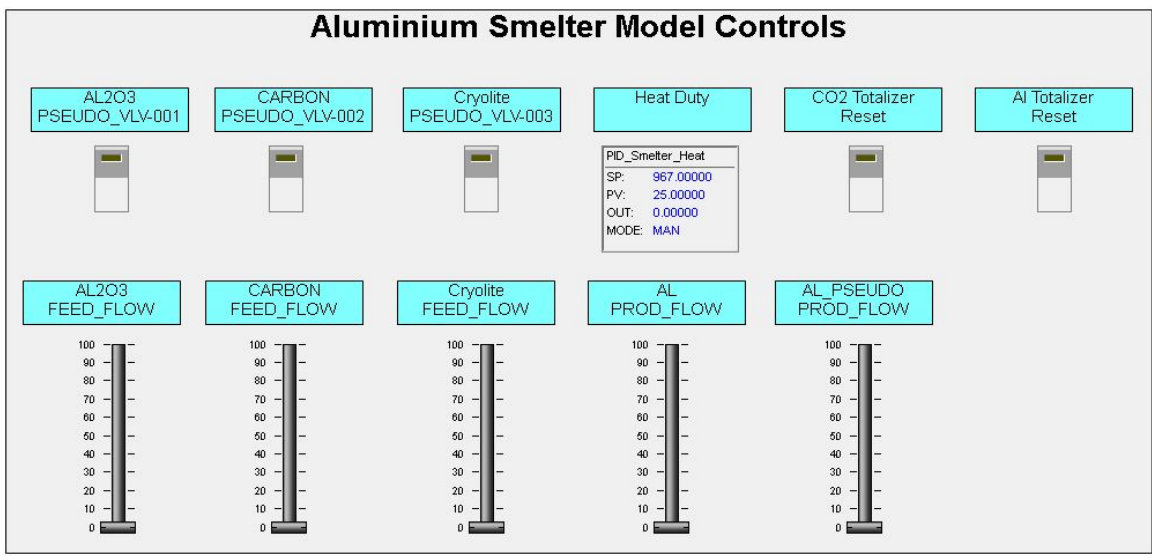


Figure 3.13. Mimic Al Smelter Process Controls

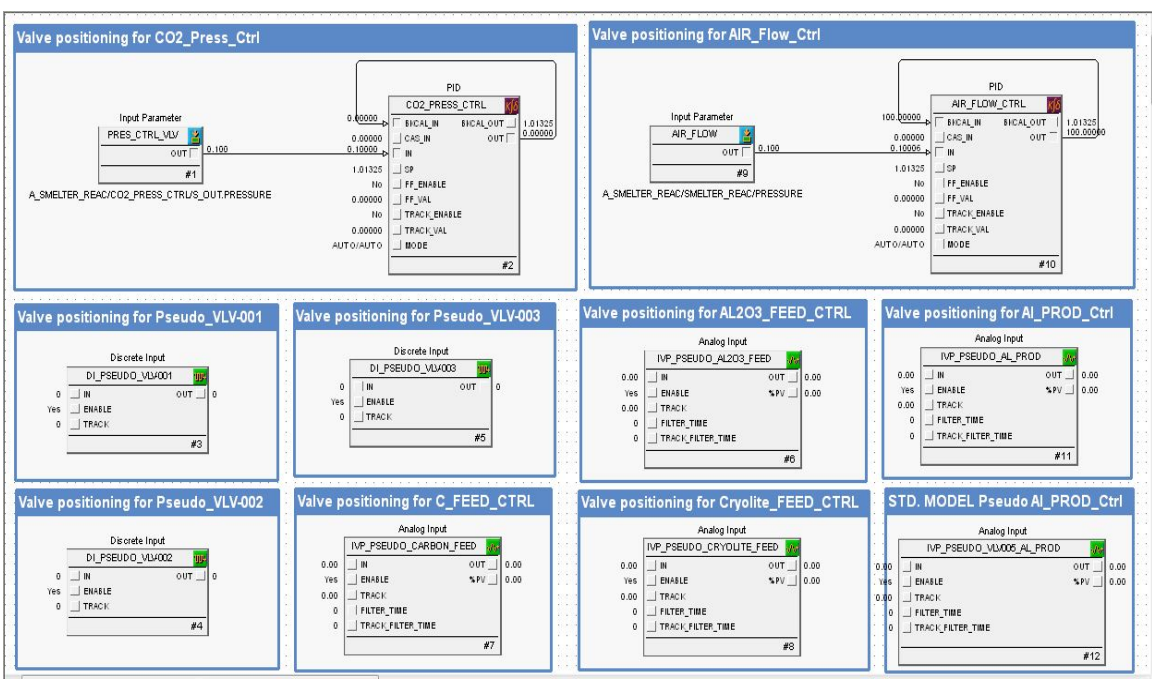


Figure 3.14. Mimic Process Control Standard Logic Models

4. SIMULATION RESULTS

Aluminum smelting is a batch process and the smelter operation simulation profile results provide a thorough understanding of the product formation, feed rates and process parameter variables. The Figure 4.1 simulation graph is directly imported from the Miimc Simulator and the process values are monitored.

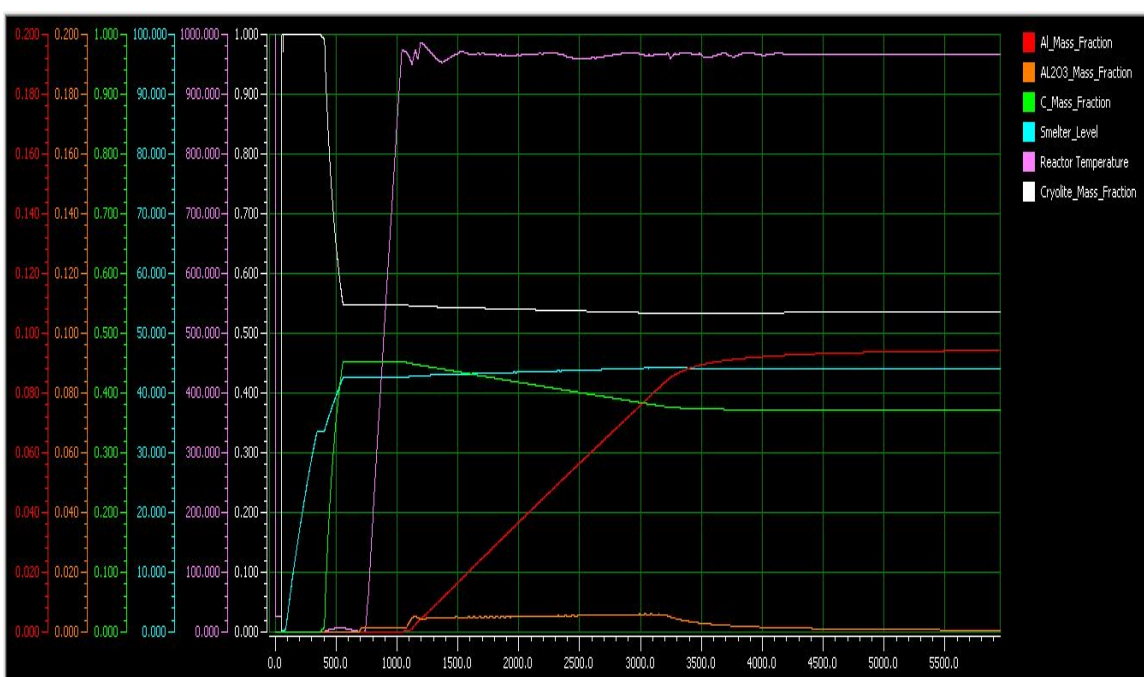


Figure 4.1. Aluminum Smelter Operating Profile Simulation Results

The electrochemical reaction is kinetically modeled with no ionization effect and chemical equilibrium is a function of temperature. The Figure 4.1 result reflects the initial stage of feeding in the smelter, the sharp increment in the aluminum production rate as soon as aluminum oxide fed into the system after maintaining process temperature and then becomes steady after it reaches to equilibrium. The liquid aluminum formation continues until the aluminum oxide completely consumed from the smelter. The

temperature is maintained in between 963–970°C by providing electrical heat energy in kW. Figure 4.2 and 4.3 shows the details of Aluminum Smelter process composition.

Integrator			
AL2O3_INT_TOTAL			
0.000 kg/min	<input type="checkbox"/> INT_IN1	TOTAL	10009.6588 kg
0.000 kg/min	<input type="checkbox"/> INT_OUT1	%TOTAL	1.0010E-007 %
No	<input type="checkbox"/> RESET	EMPTY	1.0000E+013 kg
		%EMPTY	100.0000 %
#39			

Figure 4.2. Al₂O₃ quantity fed for the simulation

Parameter	Value
Vapor_Molar_Holdup (kmol)	0.423187
Overall_Molar_Holdup (kmol)	2055.766161
Liquid_Molar_Holdup (kmol)	2055.342974
Heavy_Liquid_Molar_Holdup (...)	0.000000
Total_Vessel_Volume (m ³)	75.886491
Current_Heavy_Liquid_Volume...	0.000000
H_M_s (Btu/lbmol)	-185162.933196
H_s (Btu/lbmol)	-149119.662188
H_s (Btu/lbmol)	-185170.354685
Reactor_Level (m)	4.654443
Reactor_Percent_Height (%)	43.992847
Reactor_Percent_Volume (%)	43.992847
Heavy_Liquid_Level (%)	0.000000
Sight_Glass_Percent_Height (%)	37.871792
Sight_Glass_Percent_Volume (%)	43.992847
Liquid_Volume (m ³)	33.384628
Spec_Heat_Loss (kW/[oC kmol])	0.003316
External_Heat_Duty (kW)	6423.170537
Enthalpy_Correction (Btu/lbmol)	0.000000
Q_Agit (kW)	0.000000
Q_Jacket (kW)	0.000000
Q_Loss (Btu/lbmol)	0.335739
Time_Step (sec)	0.250000
Composition_Details	Liquid
Component_Set_Name	AL_PLANT
ALUMINUM_AL	0.095445
CARBON_C	0.369633
ALU_OXIDE_AL2O3	2.437740E-005
CARBON DIOXIDE	3.241170E-006
SOD_FLUORIDE_NAF	0.458481
ALU_FLUORIDE_ALF3	0.076413
NITROGEN	2.591050E-026
OXYGEN	4.849725E-027
CARBON MONOXIDE	0.000000
Errors	Innef

Figure 4.3. Al Smelter Final Product Composition

The Yield Calculation for this real-time dynamic simulation model as follows:

10,009.68 kg of Al₂O₃ fed to the Smelter

Al₂O₃ quantity = 10,009.68 kg = 98.173 kmol

Based on this quantity, Theoretical Al production = 196.345 kmol = 5,297.4 kg and

CO₂ generation = 147.258 kmol = 6,479.352 kg

Simulation Results after running for 24 hours, the final composition of Smelter in the liquid mole fraction is as shown in the Table 4.1. The final smelter liquid volume = 33.385 m³ and mixture liquid density = 1,868.894 kg/ m³.

Reaction Conversion or Process Yield = (Actual mol % / Theoretical mol %) * 100

$$= (9.5445 / 11.941) * 10 = 79.93\%.$$

Actual CO₂ generated = 6,462.13 kg.

Table 4.1. Theoretical and Actual (simulation) Results

Components	MW (kg/kmol)	Theoretical (kg)	Theoretical (kmol)	Theoretical Mole %	Simulation Mole % (liquid)	Reaction Conversion or Yield
Al	26.98	5,297.4	196.345	11.941	9.5445	79.93%
C	12	1,767.096	147.258	8.96	36.96	
Al ₂ O ₃	101.96	10,009.68	98.173	5.97	0	
CO ₂	44	6,479.352	147.258	8.96	0	
NaF	41.99	37,980	904.5	55.11	45.85	
AlF ₃	83.98	12,660	150.75	9.17	7.64	
N ₂	28.01	0	0	0	0	
O ₂	32	0	0	0	0	
CO	28.01	0	0	0	0	

5. ECONOMIC ANALYSIS

The aluminum industry in the United States in 2014 produced 1.72 million metric tons of primary aluminum, worth 3.97 billion dollars, at nine primary aluminum smelters. The United States was the world's 6th largest producer of primary aluminum in 2014. The Figure 5.1 shows a general PowerSim stock and flow base model for economic analysis of Primary Aluminum production in U.S.

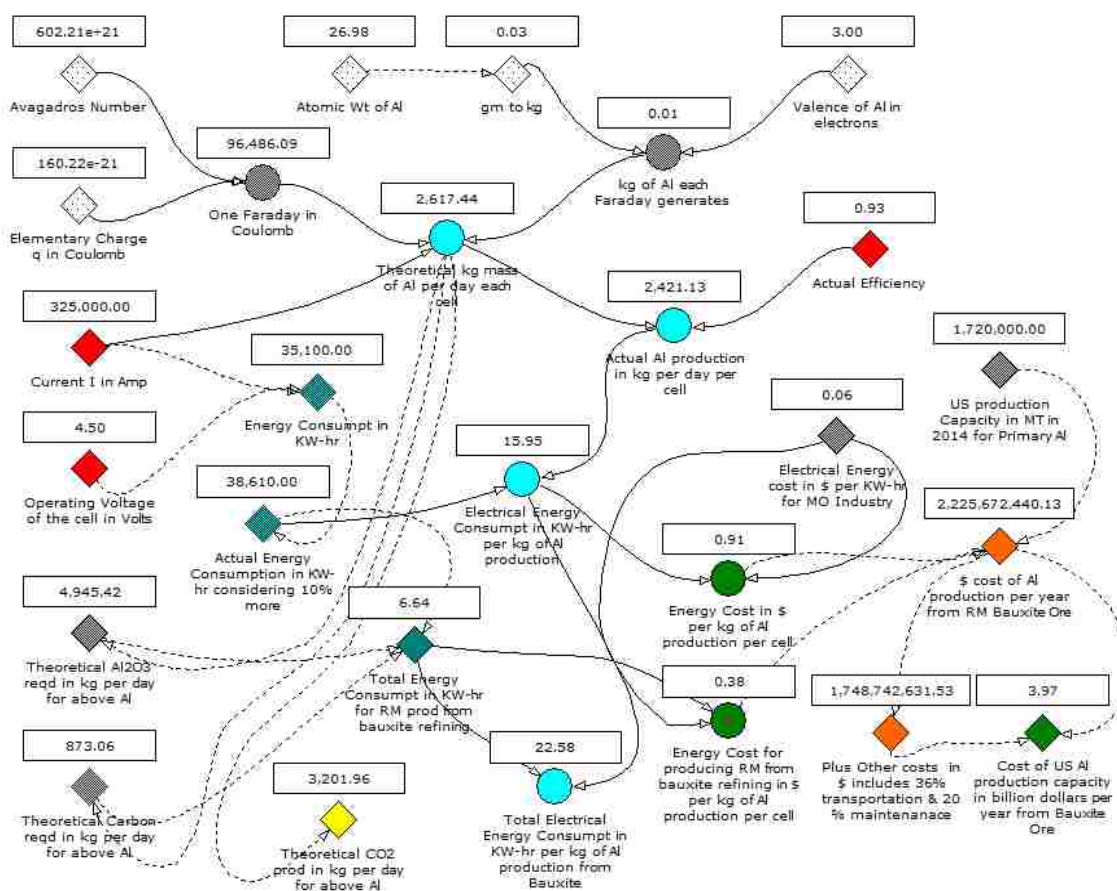


Figure 5.1. A general PowerSim stock and flow base model for economic analysis of Primary Al Production in the US

6. CONCLUSION AND FUTURE WORK

A Dynamic Simulation Model of an Aluminum Smelter has been developed using Mimic Process Simulator software to understand and analyze the operating structure of the electrolytic reduction cell, electric heat energy requirement and electrolytic reaction kinetics and mechanism of the reaction. The overall process cell model provides a good representation of the physical system, at normal operating conditions, with respect to the main operational parameters and provides a useful tool for studying various process interactions, which may aid in future improvement to existing operating and control strategies. This model can help to identify the process area where significant energy reductions and environmental impact improvement can be made to optimize and improve the process efficiency.

The model was constructed with a general cell design specification. The dynamic cell energy balance model is constructed using Mimic Software standard model with programming and then applied to this aluminum smelter, which analyzes the dynamic electrical heat energy requirement to the cell and helps to reduce the heat losses in the system. The results of this research work simulation successfully demonstrate the behavior of the electrolytic cell and the control system, although further coarse tuning of mass and energy requirement parameters would be more realistic based on actual experimental or industrial operating production data.

Even though the cell model developed provides a good representation of the physical system, there are many phenomena that were not taken into consideration. The further studies would be a direct continuation of the work described as

- The empirical modeling of disturbances of the alumina balance (feeding) and variation in the critical alumina concentration with impurities
- The modeling of the current distribution and magnetic fields in the cell and how they are influenced by sludge buildup and other operational disturbances
- The modeling of Aluminum fluoride side reactions, anode carbon reactions (carbon air burn, Boudouard reaction), evolution of hydrogen sulfide gas from the bath reactions.

REFERENCES

1. U. S. Energy Requirements for Aluminum Production - a historical perspective, theoretical limits and current practices. U.S. Department of Energy, Energy Efficiency and Renewable Energy, February 2007.
2. Haupin, Warren E., Principles of Aluminum Electrolysis. Essential Readings in Light Metals, Aluminum Reduction Technology, Volume 2, April 2013.
3. Welch, B. J., Richards, N. E., Haupin, W. E., Anodic Overpotentials in the Electrolysis of Alumina. Electrolysis. Essential Readings in Light Metals, Aluminum Reduction Technology, Volume 2, April 2013.
4. Primary Aluminum production in the United States. Retrieved Statistics from:
https://en.wikipedia.org/wiki/Aluminum_industry_in_the_United_States
https://www.statistics.com/statistics/312839/primary-aluminum-in-the-united-states/Aluminum_statistical_review_for_2014
<http://minerals.er.usgs.gov/>
www.calsmelt.com/energy-environmental.html.
5. Noranda Inc. Retrieved Statistics from: 2016 News Release – Investor Information – Noranda Aluminum,
<https://cases.primeclear.com/noranda>.
6. Jessen, Stefan W., Mathematical Modeling of a Hall Heroult Aluminum Reduction Cell, Technical University of Denmark, Thesis report, September 2008.
7. Hofer, Thomas, Numerical Simulation and Optimization of the Alumina Distribution in an Aluminum Electrolysis Pot, Thesis report, March 2011.
8. <https://www.mynah.com/resources>
www.powersim.com.
9. Chase, Malcolm W. Jr., JANAF Thermochemical Tables, 3rd Edition, Washington DC: American Chemical Society, 1985.
10. Antile, Jacques, A cell Simulator for optimizing the operation practices and the process control.

II. A HIGH TEMPERATURE STEAM/CO₂ CO-ELECTROLYSIS FOR THE UTILIZATION OF CARBON DIOXIDE FROM ALUMINUM SMELTING PROCESS FOR THE PRODUCTION OF SYNTHETIC GAS

ABSTRACT

With the increasing energy demand, decrease of the availability of cheap electricity and the need to reduce greenhouse gases emission, high temperature Steam/CO₂ Co-electrolysis (HTCE) unit has been proposed due to its impressive performance on operation efficiency, economic aspects and environmental impacts. By coupling a nuclear power small modular reactor (SMR) with the HTCE unit, the emitted carbon dioxide was used to generate Syngas through steam electrolysis and reverse water gas shift reaction. A Mimic Dynamic Simulation model has been developed to evaluate the potential performance of this process.

A high temperature Steam/CO₂ Co-electrolysis using solid oxide electrolytic cell process offers a feasible and environmentally benign technology to convert carbon-free or low-carbon electrical energy into chemical energy stored in Syngas. In this paper, a feasibility and implementation of this process is performed through process modeling and simulation. As an energy-intensive process, the cost-effective electricity is crucial and nuclear power electricity source, with which Syngas could be produced at a cost comparable to other processes.

1. INTRODUCTION AND BACKGROUND

A high temperature Co-electrolysis of steam and carbon dioxide using solid-oxide electrolytic cell (SOEC) is complicated by the fact that reverse shift reaction occurs concurrently with the electrolytic reduction reaction. Co-electrolysis significantly increases the yield of Syngas over reverse water shift reaction equilibrium composition. The process appears to be a promising technique for large-scale Syngas production.

A Mimic dynamic simulation study has been completed to assess the performance of single solid oxide electrolysis cells operating over a temperature range of 790 - 810 °C in the co-electrolysis mode, simultaneously electrolyzing steam and carbon dioxide for the production of Syngas. The simulations were performed over a range of inlet flow rates of steam, carbon dioxide, hydrogen and nitrogen using yttria-stabilized zirconium (YSZ) electrolyte. Cell operating temperature is controlled by cell potentials (voltage) and current as shown in Figure 1.1. The model prediction of outlet gas composition is based on an effective equilibrium temperature, kinetics and mechanism of the reactions.

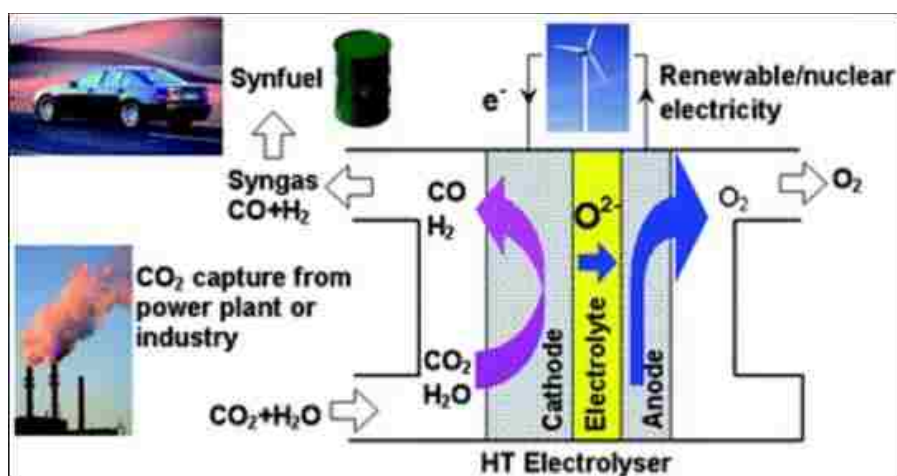


Figure 1.1. Solid Oxide Electrolysis Cell (SOEC) for Steam/ CO_2 Co-electrolysis [1]

Motivation of this Research Study:

In a power plant, the level of CO₂ emission is dependent on the nature of the fossil fuel that is used to generate electricity. Coal burning power plants emit 1.0 kg-1.1 kg of CO₂ per Kilowatt-hour (KWh) of electricity produced, while gas fired plants emit 0.35 kg – 0.4 kg CO₂ per KWh. By comparison, hydroelectric or nuclear plants do not emit significant CO₂. Therefore, CO₂ emissions per ton of aluminum produced can range from approximately 16 tons CO₂ (if coal is used), down to 5.7 tons CO₂ (if natural gas is used). If an aluminum smelter is purchasing its electricity requirements from the grid, the electricity is likely to be generated from mixture of resources.

According to IAI, there has been about 10% reduction in average energy consumption since 1990, although the rate of progressive reduction has dropped significantly in recent years. In the thermochemical processes, the chemical reaction for aluminum production is the direct source of CO₂ as shown in Figure 1.2, while the electricity required to carry out the reaction is an indirect source.

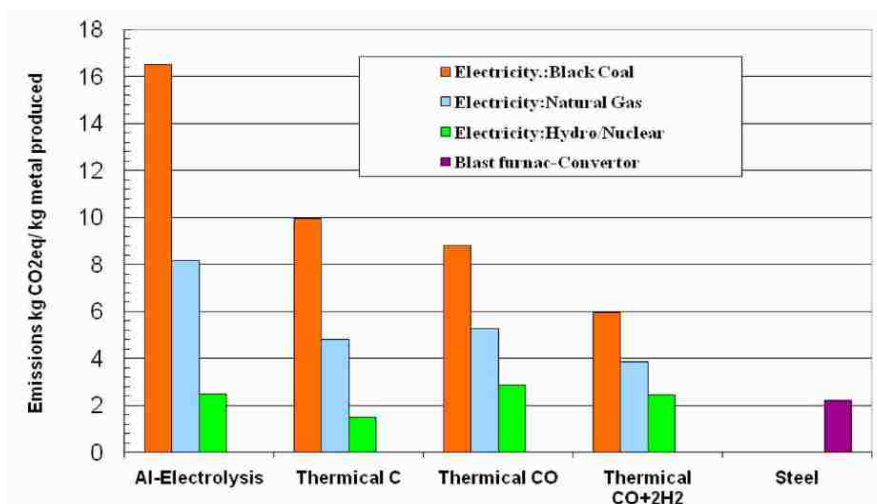


Figure 1.2. CO₂-eq emissions for current electrolysis and thermochemical processes [15]

Production of Syngas or Synfuels from Carbon dioxide and nuclear power is a “Win-Win” clean technology as shown in Figure 1.3. The U.S. currently releases 1,900 million metric tons (MMt) of CO₂ into the environment each year during production of electricity from coal, and another 1,800 MMt/year by consumption of hydrocarbon transportation fuels. Capture of CO₂ from electric power production and use of it to produce synthetic hydrocarbon transportation fuels (Synfuels) to replace petroleum-based fuels could cut this CO₂ release in half. Preliminary analysis of the CO₂ to Synfuel concept indicates CO₂ could be captured from existing fossil-fired electric plants by oxy-firing and condensing the water. CO₂ and Steam can be converted to Syngas by steam electrolysis and reverse water gas shift reaction to get CO and H₂. The Syngas can be converted to synthetic hydrocarbon transportation fuels through Fisher-Tropsch reaction.

If the carbon dioxide released by coal-fired electricity produced were converted to Synfuels, all transportation fuel could be met, and the CO₂ produced from these two sources (roughly 2/3 of US production) could be cut in half. Preliminary economic evaluation indicates that with a modest tax on release of CO₂, the cost of producing Synfuel could be comparable to current transportation fuel costs (~\$2 - \$4/gallon).



Figure 1.3. One Technology - Multiple modes of operation [4]

2. METHODOLOGY

The working mechanism of a Solid Oxide Electrolytic cell (SOEC) for the Co-electrolysis of H_2O and CO_2 are schematically shown in Figure 2.1. As driven by the externally applied D.C. voltage, oxygen ions (O^{2-}) are pumped from the cathode (Ni/YSZ cermet) side, through the solid oxide (yttria-stabilized zirconia, YSZ) electrolyte to the anode (LSM/YSZ) side (LSM is Lanthanum strontium manganese).

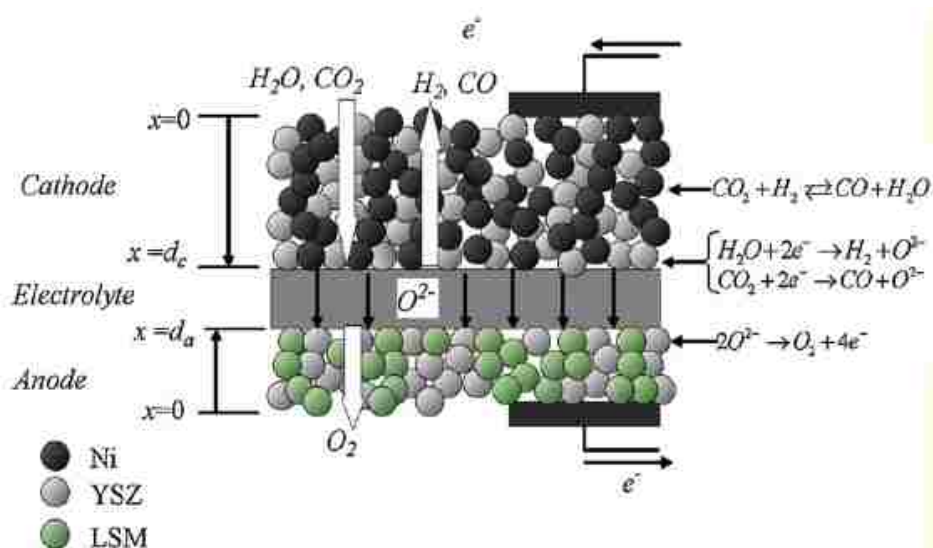
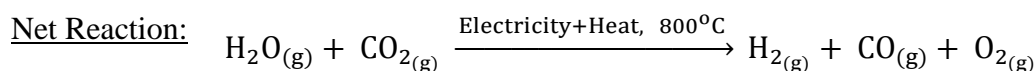
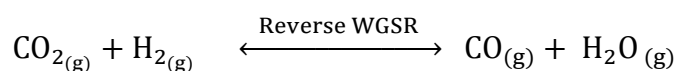
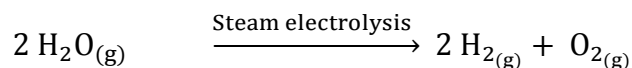


Figure 2.1. Working Mechanism of SOEC for Co-electrolysis of H_2O and CO_2 [9]

The principle of Co-electrolysis is based on steam electrolysis and reverse water gas shift reaction, which are given by following equation (1), (2) and (3) respectively,



At the cathode, H_2O and CO_2 are reduced to H_2 and CO and at the anode, oxygen ions are oxidized to oxygen. Beside the electrochemical reactions at both electrodes, the most important reactions which occur in parallel are the reverse water gas shift (RWGS) reaction. At high temperatures, RWGS is a kinetically fast, equilibrium reaction. It is heterogeneous catalytic reaction in the presence of solid catalyst such as Ni in the Ni/YSZ electrode.

To split Steam and CO_2 in high temperature Co-electrolysis, energy must be supplied to the system because of endothermic nature of the reaction. The total energy for the reaction is composed of electrical energy and thermal energy. The energy demand as a function of temperature for the high temperature Co-electrolysis is shown in Figure 2.2.

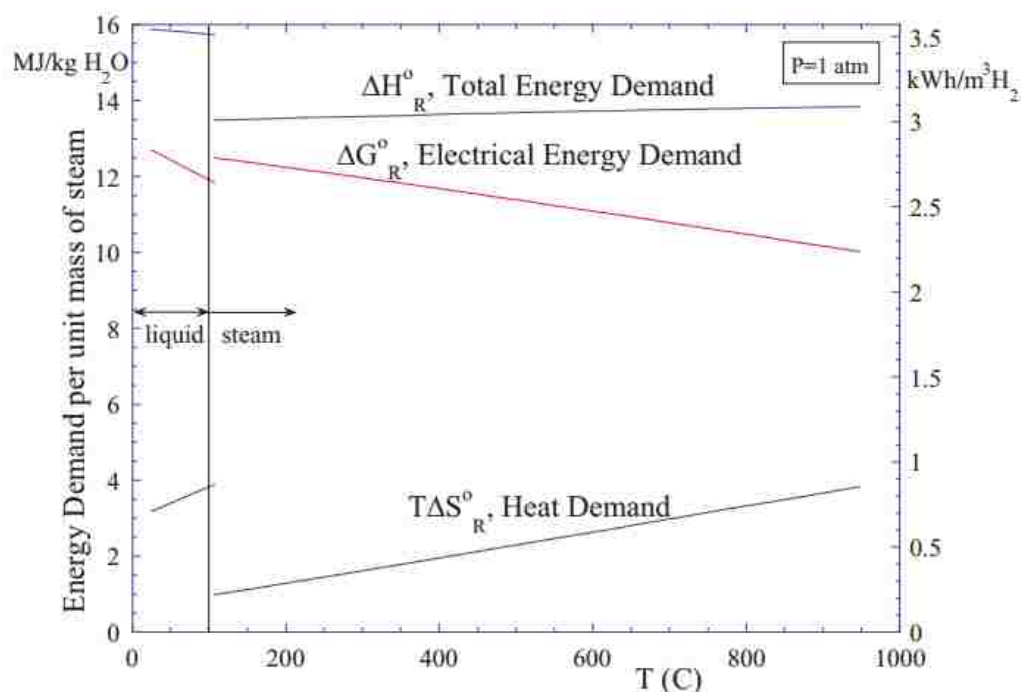


Figure 2.2. Energy Demand for High Temperature Co-electrolysis [4]

The corresponding cell voltage, in order to supply certain amount of energy (indicated by the right axes in the diagram), is correlated to the energy according to the equation: $V = W / (n \cdot F)$, where V is voltage in volt, W is the energy in J/mol and F is Faraday's constant (96,485 Coulomb/mol).

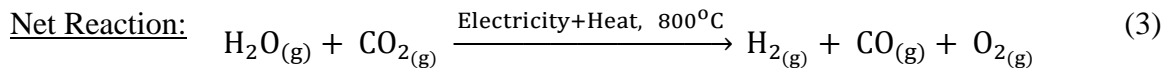
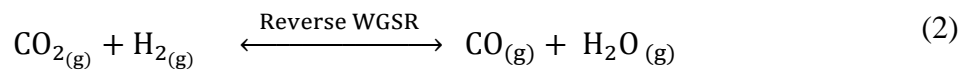
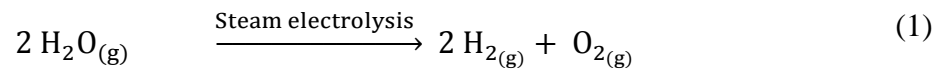
At 25⁰C, the total energy required by the reaction (3) corresponds to a voltage of 1.38 V. This voltage can be regarded as the overall thermo-neutral voltage, representing the total electrical energy required for the split of CO₂ and H₂O (with a ratio of CO₂:H₂O = 1:2) with both feedstock and product temperature at 25⁰C and without any heat energy input to the system. The step of the energy curve at 100⁰C is attributed to the evaporation heat of water (equivalent to 0.14 V). From 100 to 800⁰C, the (minimum) electricity demand decreases significantly (by 19.2%) and the (maximum) heat demand increases accordingly with increasing temperature, while the total energy demand remains essentially unchanged. Therefore, in comparison to low-temperature electrolyzer (alkaline and proton-exchange membrane electrolyzer), high-temperature solid oxide electrolyzer has a potential to reduce remarkably the specific electricity consumption per unit of product. This feature translates into significantly reduced energy cost as heat energy is usually much cheaper than electrical energy.

In principle, Syngas could be produced by separate electrolysis of steam and CO₂. The best way to carry out Co-electrolysis is to produce H₂ by high-temperature steam electrolysis, then convert the CO₂-H₂ mixture to Syngas through the RWGS reaction. Apparently the present steam/CO₂ co-electrolysis process offers an advantage of simplified system design since Syngas is in situ formed at the cathode of the electrolyzer cell and a second reactor is not required.

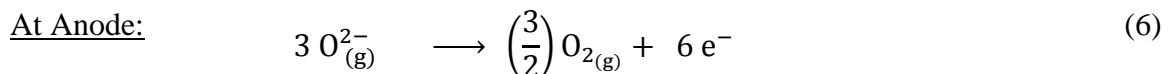
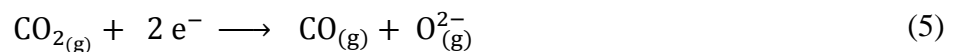
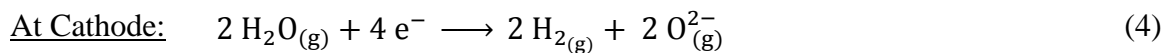
3. MIMIC DYNAMIC SIMULATION

3.1 PRINCIPLES OF HIGH TEMPERATURE CO-ELECTROLYSIS

The Net electrochemical reaction of high temperature Co-electrolysis is based on steam electrolysis and reverse water gas shift reaction shown as



At the cathode, H₂O and CO₂ are reduced to H₂ and CO and at the anode, oxygen ions are oxidized to oxygen as:



Modeling Principles & Approach:

- 1) Ionization effects of the chemical compounds and electrolytes are not considered.
- 2) The diffusion of O₂ through Ni-YSZ (Nickel - yttria stabilized zirconia) electrolyte is not modeled.
- 3) Dissociation rate of Steam and CO₂ is kinetically dependent on activation energy and concentration.
- 4) Dynamic Electrical heating is provided to the electrolytic reduction pot.
- 5) Reaction temperature, pressure and volume variables are dynamic.

- 6) Equilibrium Constant is varying with respect to temperature.
- 7) Initial condition for Syngas reactor are ambient (i.e. 1 atm and 25⁰C temp.).

The Heat of reaction for high temperature Co-electrolysis based on steam electrolysis and carbon dioxide electrolysis is calculated by the equation

$$\Delta H_{(\text{reaction,SE})}^0 = \Delta H_{(\text{product})}^0 - \Delta H_{(\text{reactant})}^0 \quad (7)$$

$$= [(\Delta H_{(\text{H}_2)}^0) + (0.5 * \Delta H_{(\text{O}_2)}^0)] - [(\Delta H_{(\text{H}_2\text{O})}^0)] \quad (8)$$

$$= [(0) + (0.5 * 0)] - [(-248.468)]$$

$$= + 248.468 \text{ kJ/mol}$$

$$\Delta H_{(\text{reaction,CE})}^0 = [(\Delta H_{(\text{CO})}^0) + (0.5 * \Delta H_{(\text{O}_2)}^0)] - [(\Delta H_{(\text{CO}_2)}^0)] \quad (9)$$

$$= [(-112.586) + (0.5 * 0)] - [(-394.838)]$$

$$= + 282.252 \text{ kJ/mol}$$

$$\Delta H_{(\text{cell,SOEC})}^0 = \Delta H_{(\text{reaction,SE})}^0 + \Delta H_{(\text{reaction,CE})}^0 \quad (10)$$

$$= 248.468 + 282.252$$

$$= + 530.720 \text{ kJ/mol}$$

As ΔH of the reaction is positive in all above reactions, it means that reactions are endothermic and Electrical plus heat energy is being provided to SOEC system. The reaction enthalpy consists of two terms

$$\Delta H = \Delta G + T * \Delta S$$

Where, ΔG is the Gibbs free energy change which has to be provided in the form of electrical energy, while the entropy part $T * \Delta S$ can be supplied as heat energy to the SOEC system. The Gibbs free energy change for high temperature Co-electrolysis at 800⁰C based on steam electrolysis and carbon dioxide electrolysis is calculated as

$$\Delta G_{(\text{reaction,SE})}^0 = \Delta G_{(\text{product})}^0 - \Delta G_{(\text{reactant})}^0 \quad (11)$$

$$= [(\Delta G_{(\text{H}_2)}^0) + (0.5 * \Delta G_{(\text{O}_2)}^0)] - [(\Delta G_{(\text{H}_2\text{O})}^0)] \quad (12)$$

$$= [(0) + (0.5 * 0)] - [(-187.035)]$$

$$= + 187.035 \text{ kJ/mol}$$

$$\Delta G_{(\text{reaction,CE})}^0 = [(\Delta G_{(\text{CO})}^0) + (0.5 * \Delta G_{(\text{O}_2)}^0)] - [(\Delta G_{(\text{CO}_2)}^0)] \quad (13)$$

$$= [(-209.075) + (0.5 * 0)] - [(-396.001)]$$

$$= + 186.926 \text{ kJ/mol}$$

$$\Delta G_{(\text{cell,SOEC})}^0 = \Delta G_{\text{f}(\text{product})}^0 - \Delta G_{\text{f}(\text{reactant})}^0 \quad (14)$$

$$= [(\Delta G_{\text{f}(\text{H}_2)}^0) + (\Delta G_{\text{f}(\text{CO})}^0) + (\Delta G_{\text{f}(\text{O}_2)}^0)] - [(\Delta G_{\text{f}(\text{H}_2\text{O})}^0) + (\Delta G_{\text{f}(\text{CO}_2)}^0)] \quad (15)$$

$$= + 373.961 \text{ kJ/mol}$$

Where, the free energies of formation of H₂ and O₂ are zero because they are pure elements and free energies of CO, H₂O and CO₂ are taken from JANAF table. As ΔG of the cell is positive, it means reaction is non-spontaneous. The minimum operating potential or voltage to accomplish the reaction is defined by Nernst Equation as

$$\Delta G_{(\text{cell})}^0 = - nFV_0 \quad (16)$$

Where, V₀ = open circuit voltage at standard conditions at 25⁰C and 1 atm

n = number of moles of electrons per mol of products

F = Faraday's constants = 96485 Coulombs*^{mol}-¹

The larger the value of the Standard reduction potentials (E⁰), the easier it is for the element to be reduced (accept electrons). In other words, they are better oxidizing agents.

$$V_{0(\text{reaction,SE})} = (-\Delta G_{(\text{reaction,SE})}^0)/nF \quad (17)$$

$$\begin{aligned}
&= (-187035 \text{ J/mol}) / ((2)*96485 \text{ J/gm.eq.volt}) \\
&= -0.969 \text{ V}
\end{aligned}$$

$$\begin{aligned}
V_{0(\text{reaction,CE})} &= (-\Delta G_{(\text{reaction,CE})}^0) / nF & (18) \\
&= (-186926 \text{ J/mol}) / ((2)*96485 \text{ J/gm.eq.volt}) \\
&= -0.969 \text{ V}
\end{aligned}$$

$$\begin{aligned}
V_{0(\text{cell,SOEC})} &= (-\Delta G_{(\text{cell,HTCE})}^0) / nF & (19) \\
&= [-(187035 + 186926) \text{ J/mol}] / ((2+2)*96485 \text{ J/gm.eq.volt}) \\
&= -0.969 \text{ V}
\end{aligned}$$

When there is no heat flux to the Solid oxide electrolytic cell (SOEC), the operating voltage is the so called Thermo-neutral voltage (or enthalpy voltage). At this voltage, the inlet and outlet temperature from a stack are equal. Although the local current densities across the cells are not identical, operation at this voltage will minimize the local temperature differences and thus mechanical stresses.

$$\begin{aligned}
V_{\text{tn}(\text{reaction,SE})} &= (-\Delta H_{(\text{reaction,SE})}^0) / nF & (20) \\
&= [(-248468) \text{ J/mol}] / ((2)*96485 \text{ J/gm.eq.volt}) \\
&= -1.288 \text{ V}
\end{aligned}$$

$$\begin{aligned}
V_{\text{tn}(\text{reaction,CE})} &= (-\Delta H_{(\text{reaction,CE})}^0) / nF & (21) \\
&= [(-282252) \text{ J/mol}] / ((2)*96485 \text{ J/gm.eq.volt}) \\
&= -1.463 \text{ V}
\end{aligned}$$

$$\begin{aligned}
V_{\text{tn}(\text{cell,SOEC})} &= (-\Delta H_{(\text{reaction,HTCE})}^0) / nF & (22) \\
&= [-(248468 + 282252) \text{ J/mol}] / ((2+2)*96485 \text{ J/gm.eq.volt}) \\
&= -1.375 \text{ V}
\end{aligned}$$

Table 3.1 shows the values of Heat of reaction, Gibb's free energy, open circuit voltages and thermo-neutral voltages for Steam Electrolysis, CO₂ Electrolysis and SOEC.

Table 3.1. Tabulated values of ΔH^0 , ΔG^0 , V_0 and V_{tn} values

	Steam Electrolysis	Carbon Dioxide Electrolysis	SOEC
$\Delta H^0_{(\text{reaction})}$ kJ/mol	+ 248.47	+ 282.25	+ 530.72
$\Delta G^0_{(\text{reaction})}$ kJ/mol	+ 187.04	+ 186.93	+ 373.96
$V_{0(\text{reaction})}$ Volts	+ 0.969	+ 0.969	+ 0.969
$V_{tn(\text{reaction})}$ Volts	+ 1.288	+ 1.463	+ 1.375

Figure 3.1 shows the operating cell potential for Co-electrolysis system using the Nernst equation for either Steam-hydrogen or for CO₂-CO at the operating temperature.

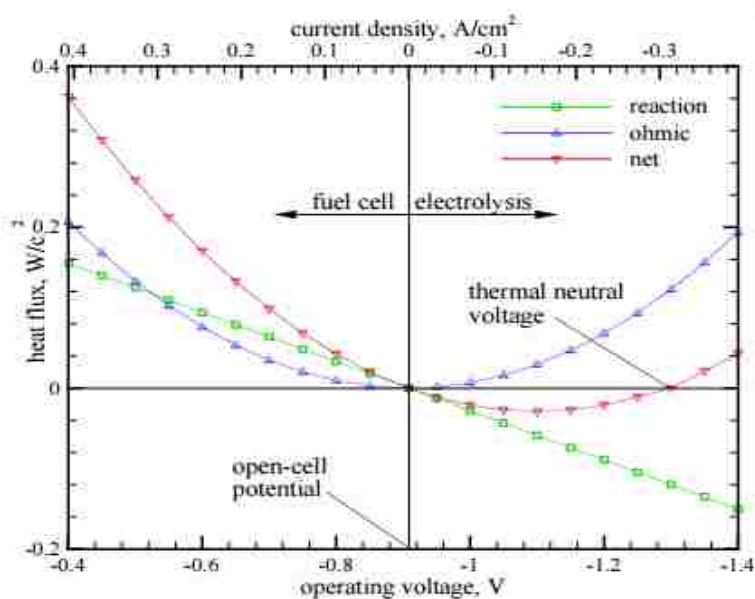


Figure 3.1. Operating cell voltage for Co-electrolysis by Idaho National Lab (INL) [4]

The Figure 3.2 shows the thermodynamics of H₂O compared to CO₂ electrolysis.

$|E|$ and U_{TNPD} are the equilibrium and thermo-neutral potential differences respectively.

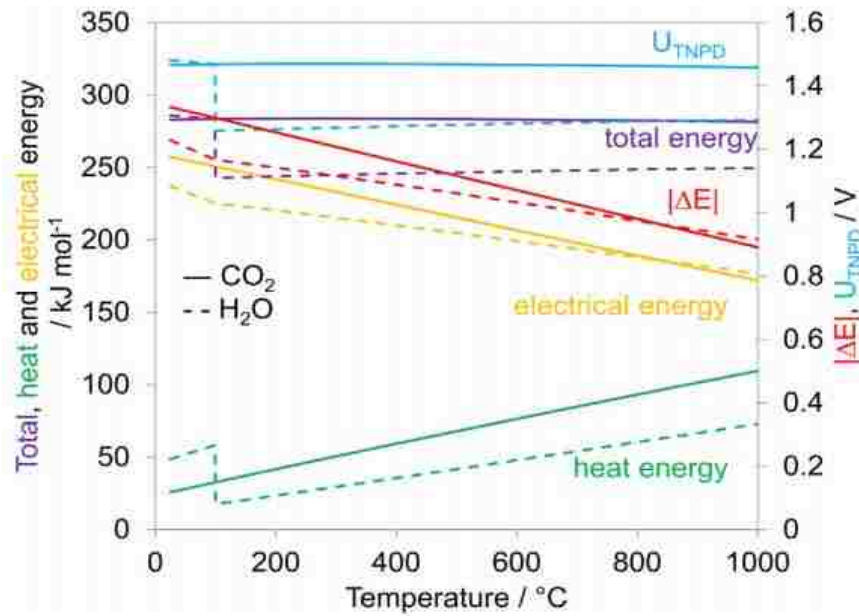


Figure 3.2. Thermodynamics of Steam/CO₂ Co-electrolysis for Syngas production [1]

The right axes show the corresponding cell voltage of the energy needed. According to Idaho National Lab, the open cell potentials for H₂O and CO₂ electrolysis are about 0.9 V. Thermal neutral voltage is the reaction voltage at which endothermic heats of reaction balance ohmic heating.

In Mimic, the equation for reaction equilibrium constant is

$$\ln K_{\text{eq}} = A_1 + \left(\frac{A_2}{T}\right) + (A_3 * \ln(T)) + (A_4 * T) \quad (23)$$

It is also evident that the equilibrium constant for high temperature Steam/CO₂ Co-electrolysis process at 800°C temperature can be calculated using relationship between ΔG^0 and K_{eq} . The standard state Gibbs free energy change is given by,

$$\Delta G^0 = -RT * \ln(K_{eq}) \quad (24)$$

As both the reactions are endothermic, the equation becomes,

$$\ln(K_{eq}) = \left(\frac{\Delta G^0}{RT} \right) \quad (25)$$

For Steam electrolysis,

$$\ln(K_{eq}) = \left(\frac{\Delta G^0}{RT} \right) = \left(\frac{(2 * 187.035) \frac{\text{kJ}}{\text{mol}}}{0.00831447 \frac{\text{kJ}}{\text{gmol} * \text{K}} * 1073 \text{ K}} \right) = 41.91$$

Therefore, it gives $A_1 = 1.606 * E+18$, $A_2 = 0$, $A_3 = 0$ and $A_4 = 0$. In the same manner,

For CO_2 electrolysis (or Reverse water gas shift reaction),

$$\ln(K_{eq}) = \left(\frac{\Delta G^0}{RT} \right) = \left(\frac{(1 * 186.926) \frac{\text{kJ}}{\text{mol}}}{0.00831447 \frac{\text{kJ}}{\text{gmol} * \text{K}} * 1073 \text{ K}} \right) = 20.95$$

It gives $A_1 = 1.254 * E+09$, $A_2 = 0$, $A_3 = 0$ and $A_4 = 0$

3.2 KINETICS AND MECHANISM OF THE REACTION

In the Idaho National Laboratory, a 3-D CFD model has been developed using FLUENT code incorporated the thermochemical reactions to perform high temperature Co-electrolysis of steam and CO_2 in a solid oxide electrolysis cell (SOEC). Co-electrolysis, however, is significantly more complex than simple steam electrolysis. This is primary due to the multiple reactions that occur: Steam Electrolysis, CO_2 Electrolysis, and Reverse Water Gas Shift reaction. Reaction kinetics govern the relative contributions of these three reactions as shown in Figure 3.3. It is also important to note that the electrolysis reactions are not equilibrium reactions since the electrolyte completely separates the products from the reactants. Therefore there is no backward reaction for

high temperature Co-electrolysis. However, the RWGSR is a kinetically fast, equilibrium reaction in the presence of a Ni Catalyst at high temperature.

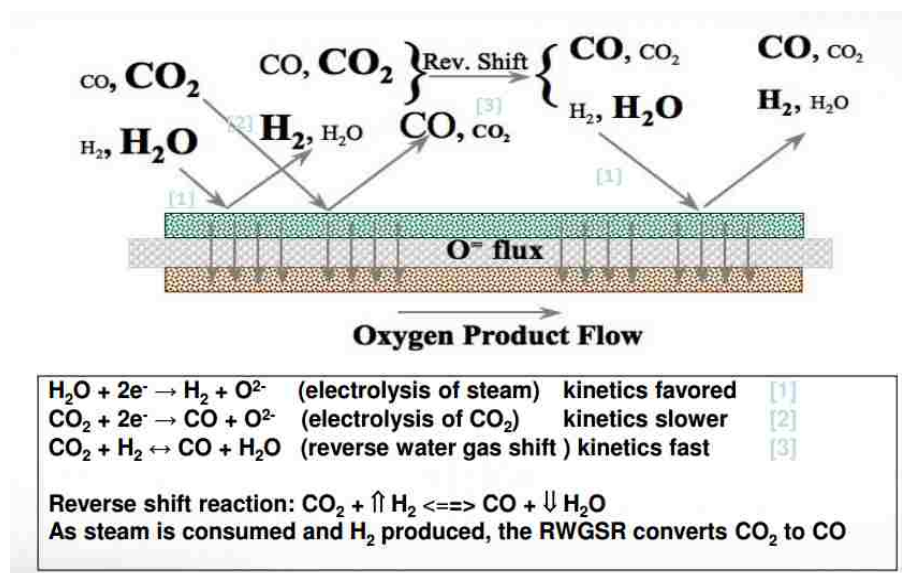


Figure 3.3. Co-electrolysis Kinetics (Reaction Paths) [7]

Experimental evidence shows that the reaction kinetics of steam electrolysis is much faster than that of the pure CO_2 electrolysis. These larger CO_2 molecules diffuse slower and create concentration overpotentials in the cell. For a given voltage, a lot more H_2 will be produced with H_2O electrolysis compared to CO produced with pure CO_2 electrolysis. The area specific resistance (ASR) of a cell is closely related to the reaction kinetics. With the assumption the reaction rate for the RWGSR is very fast (instantaneous) compared to pure CO_2 electrolysis, then this model that includes pure H_2O electrolysis with the RWGSR is a correct assumption.

The temperature dependent equilibrium constant is related to the forward and reverse reaction rates as

$$K_{eq}(T) = \frac{k_f(T)}{k_b(T)} \quad (26)$$

The net reaction rate (NRR) is defined as

$$NRR = (k_f P_{CO} P_{H_2O}) - (k_b P_{CO_2} P_{H_2}) \quad (27)$$

In FLUENT, The net rate of chemical reaction is calculated based on the molar concentration of reactants and products and not partial pressure of reactants and products as given in equation (27). To make the conversion, the ideal gas law is used as follows

$$P = \left(\frac{n}{V} * RT \right) = [C] * RT \quad (28)$$

Now the NRR can be written as

$$NRR = (k_f (RT)^2 * [C]_{CO} * [C]_{H_2O}) - (k_b (RT)^2 * [C]_{CO_2} * [C]_{H_2}) \quad (29)$$

In FLUENT, the NRR is defined as

$$NRR = (k_{f_FLUENT} * [C]_{CO} * [C]_{H_2O}) - (k_{b_FLUENT} * [C]_{CO_2} * [C]_{H_2}) \quad (30)$$

Then,

$$\begin{aligned} k_{f_FLUENT} &= k_f (RT)^2 \\ k_{b_FLUENT} &= k_b (RT)^2 \end{aligned} \quad (31)$$

An exponential curve fit of k_b versus $1/T$ from INL experiment yields

$$k_b = 4.2475 * 10^4 * \exp\left(\frac{-1.5933 * 10^4}{T}\right)$$

Applying equation (31) yields:

$$k_{b_FLUENT} = (29,359) * (T)^2 * \exp\left(\frac{-1.3247 * 10^8}{RT}\right)$$

By exponential curve fit of $k_{f_FLUENT} = k_{b_FLUENT}(T) * K_{eq}(T)$ versus $1/T$ gives

$$k_{f_FLUENT} = (390.96) * (T)^2 * \exp\left(\frac{-9.363 * 10^7}{RT}\right) \quad (32)$$

Comparing this equation with Modified Arrhenius type equation,

$$k = (A) * (T)^n * \exp\left(\frac{-E_a}{RT}\right) \quad (33)$$

It gives activation energy $E_{a(RWGS)} = 9.363 * 10^7 \frac{J}{\text{kgmol}} = 93,630 \frac{\text{kJ}}{\text{kmol}}$ and

Pre-exponential factor $A_{(RWGS)} = 390.96 \text{ sec}^{-1}$.

From IDL Literature, the equilibrium constant equation for the shift reaction is given as

$$\ln(K_{\text{eq}}(T)) = -1.24911 + \left(\frac{4.92194 * 10^3}{T}\right) + (-7.78386 * 10^{-1}) \ln(T) \quad (34)$$

$$+ (2.5559 * 10^{-3})T + (-5.0983 * 10^{-7})T^2$$

From the Figure 3.4, the activation energy for the high temperature region (above 700°C) for the steam electrolysis in the solid oxide electrolysis cell using yttria-stabilized zirconium (YSZ) electrolyte is 0.78 eV in good agreement with the experimental results.

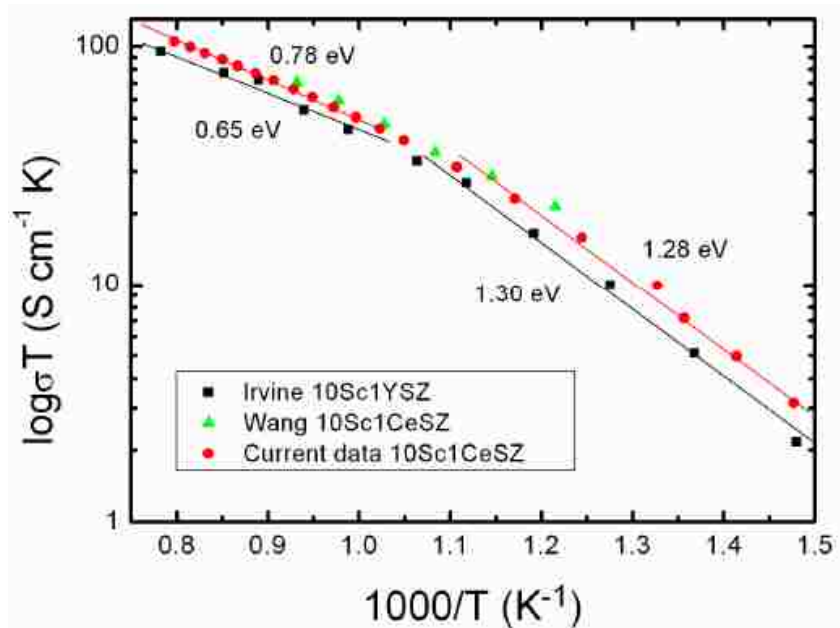
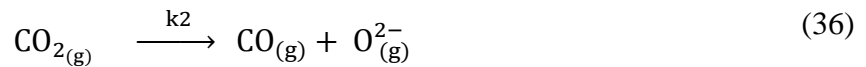
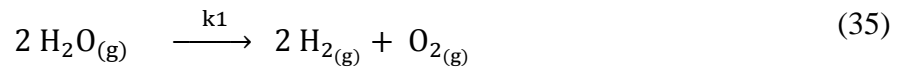


Figure 3.4. High Temperature Steam/CO₂ Electrolysis in SOEC using YSZ Electrolyte [11]

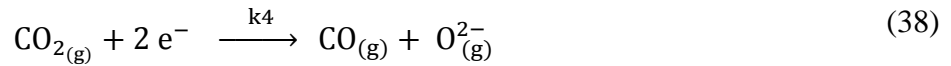
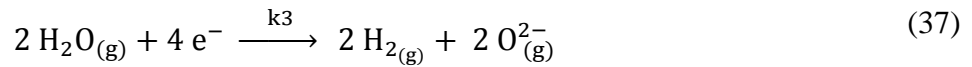
$$\begin{aligned} \text{Activation energy } E_{a(\text{SE})} &= 0.78 \frac{\text{eV}}{\text{particles of water molecule}} = (0.78 * 23.06) \frac{\text{kcal}}{\text{mol}} \\ &= (17.987 * 4.184) \frac{\text{kJ}}{\text{mol}} = 75,257.6 \frac{\text{kJ}}{\text{kmol}} \end{aligned}$$

As Steam electrolysis is kinetically fast reaction, pre-exponential factor $A_{(\text{SE})} = 0.001 \text{ sec}^{-1}$ (assumed). The measurements are carried out in the temperature range of 790⁰C to 810⁰C. The wall surrounding ambient temperature is 25⁰C. The mechanism steps for the high temperature Steam/CO₂ Co-electrolysis are given as

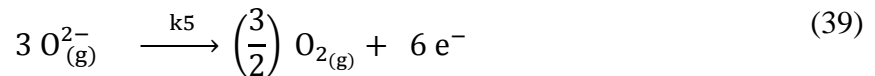
Step I) Dissociation of Steam (water gas) and CO₂ molecules



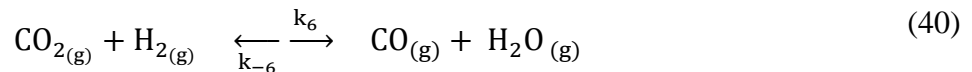
Step II) Cathodic reaction of steam and carbon dioxide ions



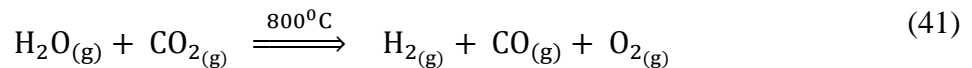
Step III) Anodic reaction of oxygen ions



Step IV) Reverse water gas shift reaction



Step V) Net reaction for the formation of carbon monoxide and hydrogen (i.e. Syngas)



Reaction I and IV are rate determining steps for Steam electrolysis and Reverse water gas shift reaction separately.

The net reaction rate, $r = r_f - r_b$ (42)

The expression for forward rate r_f of the overall reaction is

$$r_f = \left(k_{0f} * e^{\left(\frac{-E_{actf}}{RT} \right)} \right) * (\prod C_i^{a_{if}}) \quad (43)$$

$$r_f = \left(k_f * e^{\left(\frac{-E_{actf}}{RT} \right)} \right) * (C_{H_2O(g)} * C_{CO_2(g)}) \quad (44)$$

The expression for backward rate r_b of the overall reaction is

$$r_b = \frac{k_f}{K_{eq}} * (\prod C_i^{a_{ib}}) \quad (45)$$

$$r_b = \frac{k_f}{K_{eq}} * (C_{H_2(g)} * C_{CO(g)} * C_{O_2(g)}) \quad (46)$$

Where,

$$K_{eq} = (C_{H_2(g)} * C_{CO(g)} * C_{O_2(g)}) / (C_{H_2O(g)} * C_{CO_2(g)}) = \frac{k_f}{k_b} \quad (47)$$

E_{actf} (E_{actb}) = Activation energy of the forward (reverse) reaction, KJ/kmol

R = Universal gas constant, KJ/(kmol*K) = 8.314 KJ/(kmol*K)

k_f (k_b) = rate constants for the forward (reverse)

C_i = Concentration of “i” component, molar fraction or kmol/m³

a_{if} (a_{ib}) = partial order of the i component in forward (reverse) direction

Π = multiplication operator

f = characterizes the forward reaction

b = characterizes the backward reaction

K_{eq} = Equilibrium Constant

SE, CE, SOEC = Steam electrolysis, CO₂ electrolysis and Solid Oxide electrolytic cell

respectively.

3.3 MATERIAL AND ENERGY BALANCE

Material Balance:

The Aluminum Smelter plant capacity at Noranda New Madrid, MO = 260,000 MT/yr.

Average operating rate of plant = 97%, where 3% is plant breakdown and shutdown

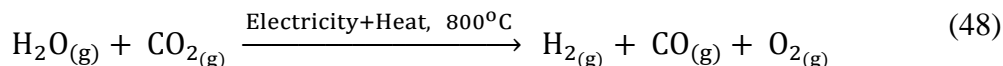
$$\begin{aligned} \text{Hence, Primary Al operating capacity} &= (0.97 * 260 * 10^6) \text{ kg/yr} = \left(\frac{0.97 * 260 * 10^6}{12 * 30 * 24} \right) \text{ kg/hr} \\ &= 29,190 \text{ kg/hr} = (31435 \text{ kg} / 26.98 \text{ kg/kmol}) \\ &= 1082 \text{ kmol} \end{aligned}$$

3 kmol of CO₂ = 4 kmol of Al, therefore for 1082 kmol of Al,

$$\begin{aligned} \text{CO}_2 \text{ produced} &= (3/4) * 1082 = 811.5 \text{ kmol} \\ &= (811.5 \text{ kmol} * 44 \text{ kg/kmol}) = 35,706 \text{ kg/hr} \end{aligned}$$

Basis: 35,706 kg/hr of CO₂ feed for the Syngas production

The net reaction for the co-electrolysis of steam and CO₂ for the production of Syngas is



$$\text{H}_2\text{O required} = 811.5 \text{ kmol} = (811.5 \text{ kmol} * 18 \text{ kg/kmol}) = 14,607 \text{ kg/hr}$$

$$\text{H}_2 \text{ produced} = (811.5 \text{ kmol} * 2 \text{ kg/kmol}) = 1,623 \text{ kg/hr}$$

$$\text{CO produced} = (811.5 \text{ kmol} * 28 \text{ kg/kmol}) = 22,722 \text{ kg/hr}$$

$$\text{O}_2 \text{ produced} = (811.5 \text{ kmol} * 32 \text{ kg/kmol}) = 25,968 \text{ kg/hr}$$

In actual practice, feed Raw Materials will be excess, hence considering 5% excess RM and kg per 30 minutes RM flow to maintain the pressure in the reactor.

$$\text{CO}_2 \text{ feed} = (1.05 * 35706 \text{ kg/hr}) = (37491.3/30) \text{ kg/min} = 1,249.72 \text{ kg/min}$$

$$\text{H}_2\text{O feed} = (1.05 * 14607 \text{ kg/hr}) = (15337.4/30) \text{ kg/min} = 511.25 \text{ kg/min}$$

$$\text{Volume} = \frac{\text{Mass}}{\text{Density}}$$

$$V_{\text{CO}_2(\text{g})} = \left(\frac{1249.72 \text{ kg}}{1.977 \frac{\text{kg}}{\text{m}^3}} \right) = 632 \text{ m}^3 \quad \text{Where, } \rho_{\text{CO}_2(\text{g})} = 1.977 \text{ kg/m}^3$$

$$V_{\text{H}_2\text{O}(\text{g})} = \left(\frac{511.25 \text{ kg}}{0.59 \frac{\text{kg}}{\text{m}^3}} \right) = 867 \text{ m}^3 \quad \text{Where, } \rho_{\text{H}_2\text{O}(\text{g})} = 0.59 \text{ kg/m}^3$$

$$\begin{aligned} \text{Total RM Volume of CSTR, } V_{\text{CSTR}(\text{RM})} &= (V_{\text{CO}_2(\text{g})} + V_{\text{H}_2\text{O}(\text{g})}) \\ &= (632 + 867) \text{ m}^3 = 1,499 \text{ m}^3 \end{aligned}$$

Considering 45% excess volume to maintain the pressure in the reactor,

$$\text{Actual } V_{\text{CSTR}(\text{Total})} = (1.45 * 1499) = 2,173 \text{ m}^3 = 76,739 \text{ ft}^3$$

Reactor Configuration:

As vessel operating pressure $0 < P < 17$ bars, recommended $L/D = 3.5$. Now, for calculating the vessel sizing, the vessel diameter is given by

$$D = \left(\frac{V_{(\text{T})}}{\left(\frac{1}{4}\right) * \pi * \left(\frac{L}{D}\right)} \right)^{1/3} \quad (49)$$

Reactor Diameter $D = 9.248 \text{ m}$, Reactor radius $r = 4.624 \text{ m} = 15.17 \text{ ft}$

Reactor Length $L = \left(D * \frac{D}{L} \right) = (9.248 * 3.5) = 32.368 \text{ m} = 106.2 \text{ ft}$

Reactor minor radius = 4 ft.

The Syngas reactor is considered to be spherical shape at both top and bottom ends. Initial Boundary Conditions: Pressure = 1.01325 atm, Temperature = 25⁰C. Figure 3.5 and 3.6 shows the Syngas reactor sizing and initial start-up configuration respectively. The activities of components are calculated based on the component phases. Table 3.2 shows Syngas reactor initial start-up feed inlet stoichiometric composition.

Reactor Configuration

Units Settings 1 Settings 2 Agitator Elevations Heat Source Composition Reaction

Reactor Type
 Vertical Horizontal

Spherical Ends
 Top Bottom

Number of Inputs (1-8) 2

Number of Outputs (1-8) 2

Reactor Radius 15.17 ft

Reactor Height 106.2 ft

Reactor Minor Radius 4 ft

Initial Conditions
 Pressure - Temp (Calc Level) Pressure - Level (Calc Temp)

Initial Temperature 25 °C

Initial Sight Glass Level 70 %

Initial Pressure 1.01325 atm

Figure 3.5. Syngas Reactor Sizing Configuration

Reactor Configuration

Units Settings 1 Settings 2 Agitator Elevations Heat Source Composition Reaction

Component Set
 AL_SYG_PLANT Change

Activity Coefficients
 External Constant

Fraction type
 Mole Fraction Mass Fraction

Solid	Component	Fraction	Activity
No	ALUMINUM_AL	0.000	0.001
No	CARBON_C	0.000	0.001
No	ALU_OXIDE_AL2O3	0.000	0.001
No	CARBON DIOXIDE	0.000	200.000
No	SOD_FLUORIDE_NAF	0.000	0.001
No	ALU_FLUORIDE_ALF3	0.000	0.001
No	NITROGEN	0.790	200.000
No	OXYGEN	0.210	200.000
No	CARBON MONOXIDE	0.000	200.000
No	WATER	0.000	200.000
No	HYDROGEN	0.000	200.000
No	METHANE	0.000	200.000
Total:		1.000	

Zero Normalize

Figure 3.6. Syngas Reactor Initial Configuration at the start-up

Table 3.2. Feed Inlet Stoichiometric Composition at the initial start-up

Components	MW (kg/kmol)	Feed Flow (kg/hr)	Feed Flow (kmol/hr)	Mass Fraction (wt %)	Mole Fraction (mol %)	Activity
Al	26.98	0	0	0	0	0.001
C	12	0	0	0	0	0.001
Al ₂ O ₃	101.96	0	0	0	0	0.001
CO ₂	44	37,491.3	852.08	0.7097	0.5003	200
NaF	41.99	0	0	0	0	0.001
AlF ₃	83.98	0	0	0	0	0.001
N ₂	28.01	1.13E-03	4.03E-05	2.14E-08	2.37E-08	200
O ₂	32	3.80E-04	1.19E-05	7.19E-09	6.97E-09	200
CO	28.01	0	0	0	0	200
H ₂ O	18.02	15,337.4	851.13	0.2903	0.4997	200
H ₂	2.016	0	0	0	0	200
CH ₄	16.043	0	0	0	0	200

Energy Balance:

The total energy ($\Delta H_R^0 = \Delta G_R^0 + T\Delta S_R^0$) associated with the high temperature Co-electrolysis of Steam and CO₂ for direct production of Syngas is shown as follows:

- ΔH_R^0 , Total energy demand = 13.5 MJ/kg H₂O (steam) or 3.1 kWh/m³ H₂
- ΔG_R^0 , Electrical energy demand = 12.5 MJ/kg H₂O (steam) or 2.2 kWh/m³ H₂
- $T\Delta S_R^0$, Heat demand = 1 MJ/kg H₂O (steam) or 0.9 kWh/m³ H₂

The ideal electrical energy require per kg of H₂ produced = 32 kWh, and combined ideal electrical energy require per kg of Syngas (CO + H₂) produced = 39 kWh.

The Syngas reactor energy calculation Mimic model shows the heat duty required to run the Syngas production solid oxide electrolytic cell in kWh as shown in Figure 3.7.

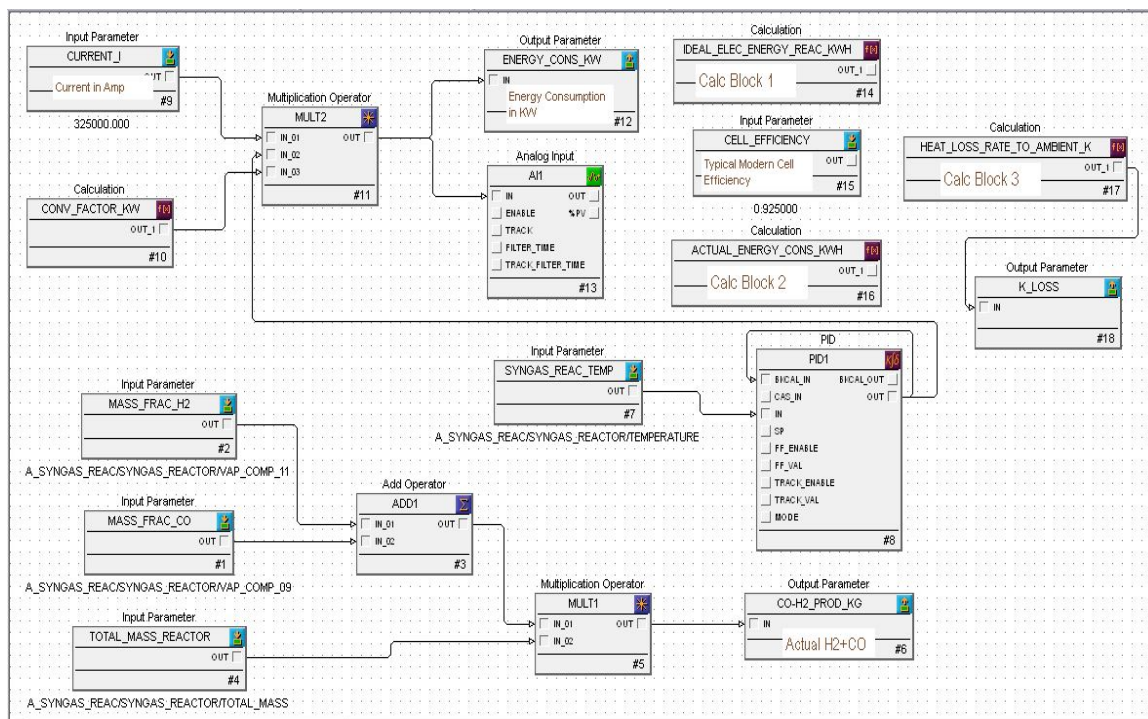


Figure 3.7. Syngas Energy Balance Mimic Standard Model

The theoretical electrical heat energy in kWh required per kg of H₂+CO produced to run the electrolytic cell at 100% efficiency is calculated and shown in Figure 3.8. The calculation for actual in-plant electrical heat energy in kWh required per kg of H₂+CO produced for the electrolytic cell at 92.5% efficiency is shown in Figure 3.9.

```

Calc Block
1 F$1 := VAL("ENERGY_CONS_KW/IN");
2     //Considering actual eff. 100 % of the cell
3
4 F$2 := F$3;
5
6 F$3 := VAL("CO-H2_PROD_KG/IN");
7
8 OUT_1 := F$1/3600/(F$3 - F$2);
9     //Electrical energy in KWh/kg of CO+H2 produced
  
```

Figure 3.8. Ideal Electrical Energy Required in KWh for Figure 3.7 Calc Block 1

```

1 F$1 := VAL("ENERGY_CONS_KW/IN")/VAL("CELL_EFFICIENCY/OUT");
2     //Considering actual eff. 92.5% of the cell
3
4 F$2 := F$3;
5
6 F$3 := VAL("CO-H2_PROD_KG/IN");
7
8 OUT_1 := F$1/3600/(F$3 - F$2);
9     //Electrical energy in kWh/kg of CO+H2 produced

```

Figure 3.9. Actual Electrical Energy Required in KWh for Figure 3.7 Calc Block 2

The electrical energy required to run the high temperature Steam/CO₂ electrolytic reaction is 39 kWh per kg of H₂+CO produced. Here, the heat losses to the surrounding need to be considered. Hence, Specific rate of Heat loss (K) of electrolytic reduction cell to ambient in kW*°C⁻¹kmol⁻¹ is calculated as shown in Figure 3.10.

```

1 F$1 := (39-37.5)/VAL("CELL_EFFICIENCY/OUT");
2     // Heat loss in kWh/kg of CO+H2 Produced
3     // Actual heat - Ideal heat
4 F$2 := F$1*3600; // Heat loss Q in KW
5 F$3 := 25; // Ambient temp in degC
6 F$4 := VAL("A_SYNGAS_REAC/SYNGAS_REACTOR/TEMPERATURE");
7     //Reactor temp in degC
8 F$5 := VAL("A_SYNGAS_REAC/SYNGAS_REACTOR/TOTAL_HOLDUP");
9     //Reactor Molar Holdup in kmols
10
11 //K(loss) = Q(loss)/ ( Ms * (Ts -Tamb) )
12
13 OUT_1 := F$2/(F$5*(F$4-F$3));
14     //K(loss) Specific heat loss rate to surrounding(ambient)

```

Figure 3.10. Specific Heat Loss Rate to the surrounding for Figure 3.7 Calc Block 3

3.4 PROCESS MODEL AND CONTROLS

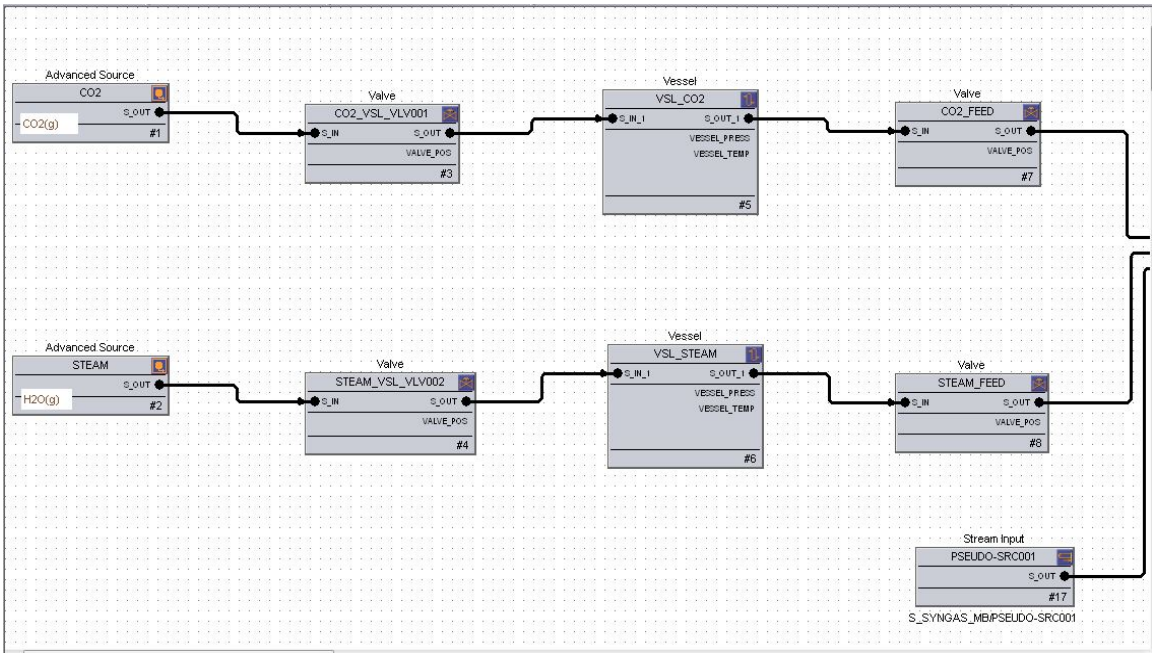


Figure 3.11. Mimic Process Feed Model

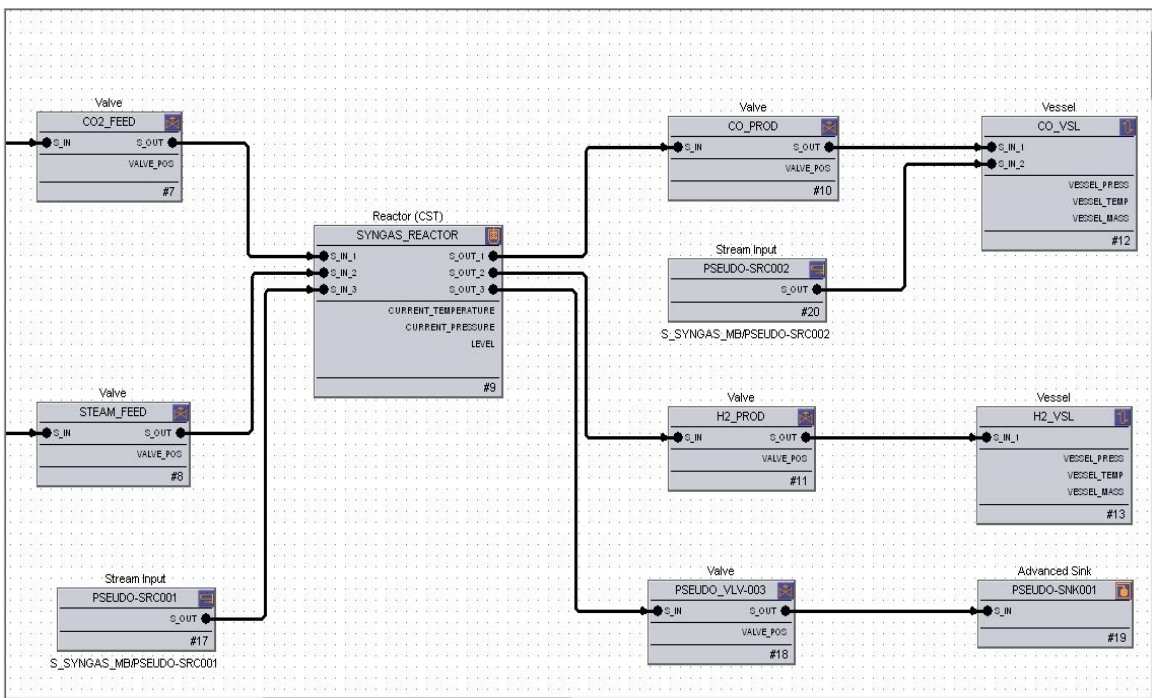


Figure 3.12. Mimic Process Model

Above Figure 3.11 and 3.12 shows the Mimic Syngas Process production model. Figure 3.13 shows the Syngas reactor process production withdrawal Mimic model for siphoning off syngas from the process and maintaining the process parameters. Figure 3.14 shows the Syngas production process operation control view.

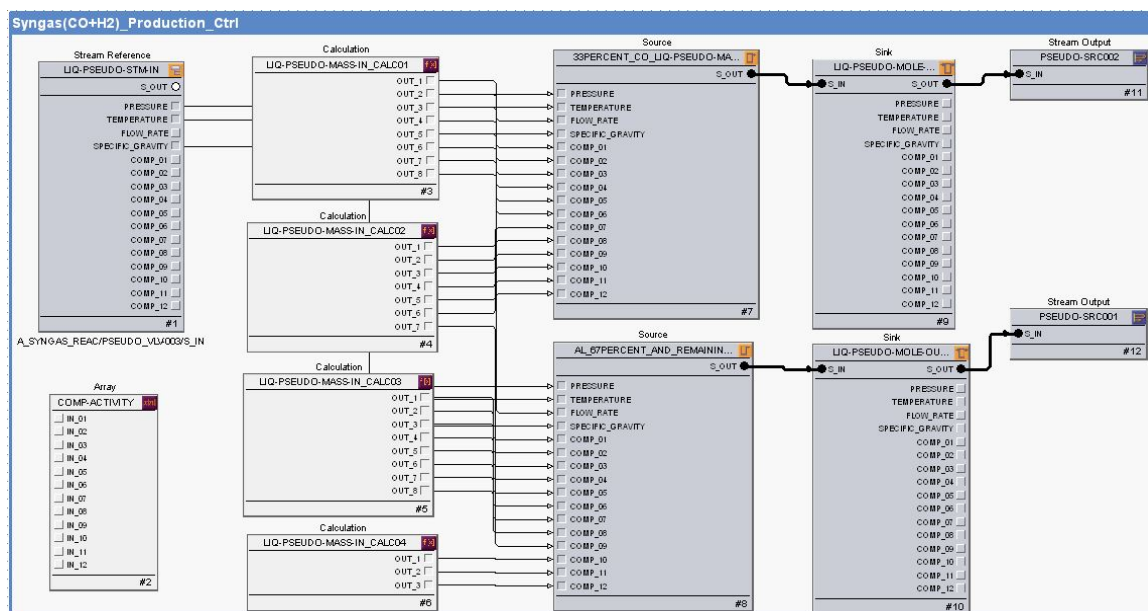


Figure 3.13. Syngas reactor Production Withdrawal Mimic Standard Model

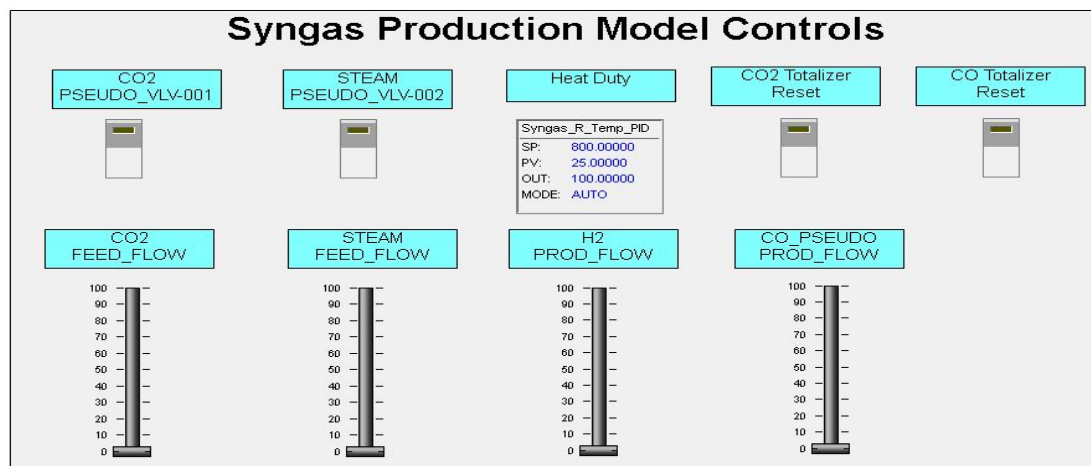


Figure 3.14. Mimic Syngas Production Process Controls

Figure 3.15 shows the Mimic Process Control Logic standard models for controlling the feed and product streams flow, temperature and pressure.

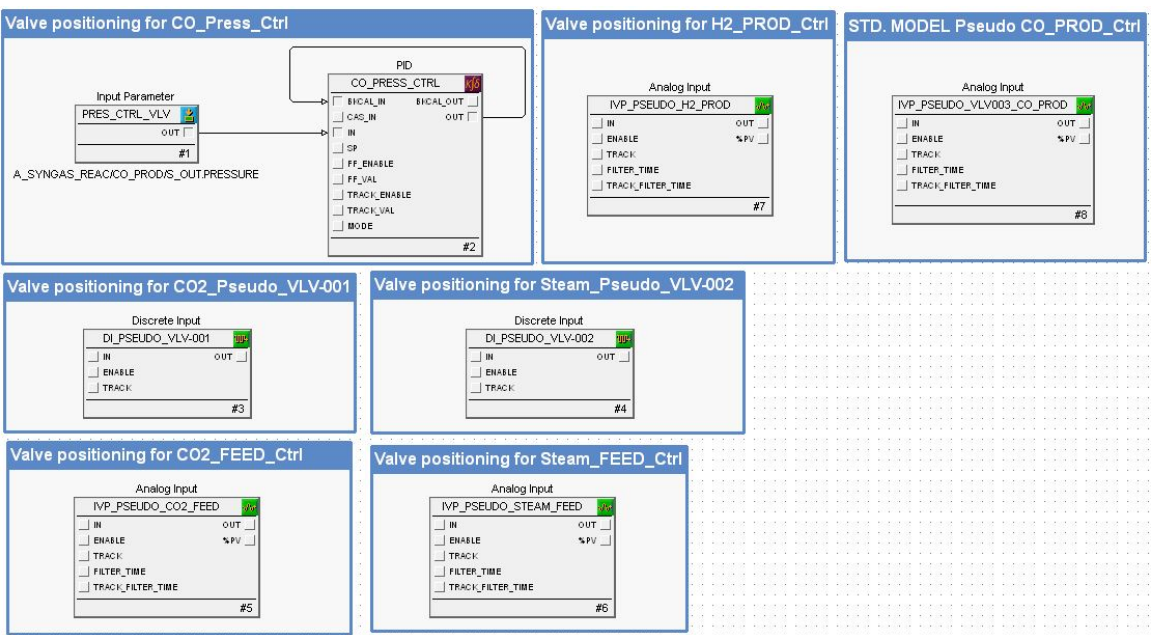


Figure 3.15. Mimic Process Control Standard Models

4. SIMULATION RESULTS

The high temperature Co-electrolysis in a solid oxide electrolytic cell is a most promising technology and the Syngas production simulation profile results provide a detailed analysis of the product formation, feed rates and process parameter variables. Figure 4.1 simulation graph is directly imported from the Miimc Simulator and the process operating values are monitored.

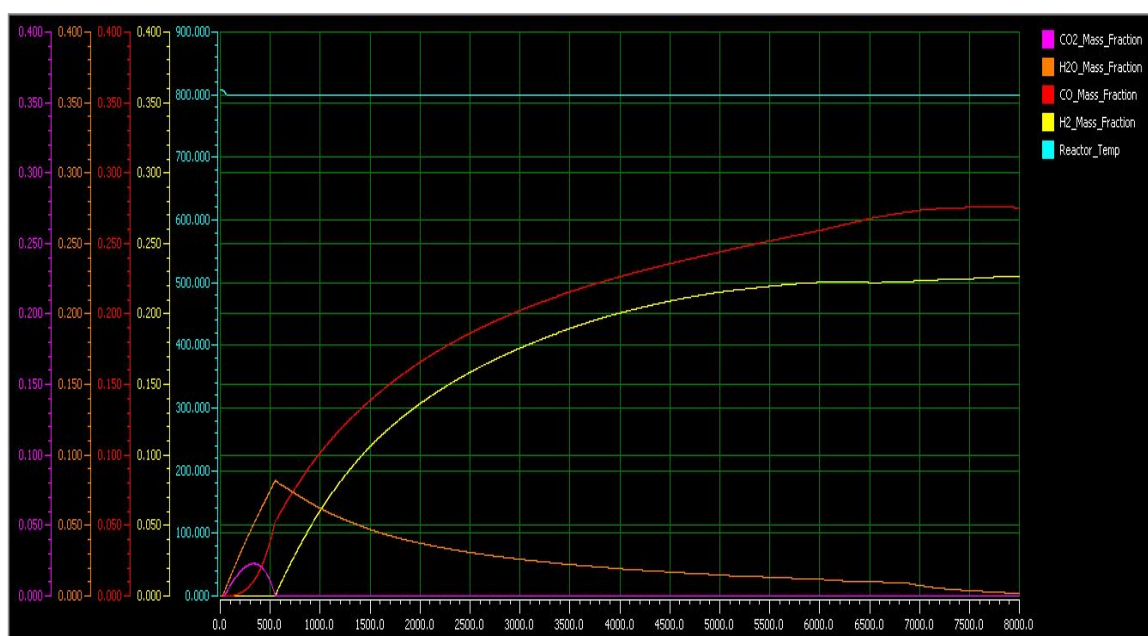


Figure 4.1. Syngas reactor Production Operating Profile Simulation Results

The electrochemical reaction is kinetically modeled with no ionization effect and chemical equilibrium is a function of temperature. The Figure 4.1 result reflects the initial stage of feeding in the Syngas reactor, the sharp increment in the CO and H₂ production rate as soon as H₂O gas and CO₂ fed into the system by maintaining process temperature and becomes steady after it reaches to equilibrium. At 6000 sec., H₂O gas flow stopped,

therefore H₂ formation rate got reduced and at 7000 sec., CO₂ gas flow stopped, therefore CO mass fraction started gradually decreasing in overall mass and H₂ gas mass fraction started gradually increasing in overall mass because RWSG reaction wouldn't work in absence of CO₂ gas feed therefore the remaining steam would just convert into H₂ gas. The H₂ gas formation continues until the steam completely consumed from the reactor. The temperature is maintained in between 790–810⁰C by providing electrical heat energy. The Syngas production reactor final process composition details and CO₂ and Steam quantity fed for the simulation are shown in Figure 4.2 and 4.3 respectively.

Parameter	Value
Description	
Values_To_Display	...
Reset	No
Temperature (°C)	800.0000
Top_Pressure (atm)	10.9675
Bottom_Pressure (atm)	10.9675
Vapor_Molar_Holdup (kmol)	270.7814
Overall_Molar_Holdup (kmol)	270.7814
Liquid_Molar_Holdup (kmol)	0.0000

Parameter	Value
Heavy_Liquid_Molar_Holdup (kmol)	0.0000
Total_Vessel_Volume (ft3)	76779.5479
Current_Heavy_Liquid_Volume (ft3)	0.0000
H_M_s (Btu/lbmol)	-2751.0003
H_s (Btu/lbmol)	-2751.0031
H_s (Btu/lbmol)	-26954.7857
Reactor_Level (ft)	0.0000
Reactor_Percent_Height (%)	0.0000
Reactor_Percent_Volume (%)	0.0000
Heavy_Liquid_Level (%)	0.0000
Sight_Glass_Percent_Height (%)	0.0000
Sight_Glass_Percent_Volume (%)	0.0000
Liquid_Volume (ft3)	0.0000
Spec_Heat_Loss (kW/(°C kmol))	0.0000
External_Heat_Duty (kW)	2.1987
Enthalpy_Correction (Btu/lbmol)	0.0000
Q_Agit (kW)	0.0000
Q_Jacket (kW)	0.0000
Q_Loss (Btu/lbmol)	0.0000
Time_Step (sec)	0.5000
Composition_Details	Overall
Component_Set_Name	AL_SYG_PLANT
ALUMINUM_AL	0.0000
CARBON_C	0.0000
ALU_OXIDE_AL2O3	0.0000
CARBON DIOXIDE	6.6400E-040
SOD_FLUORIDE_NAF	0.0000
ALU_FLUORIDE_ALF3	0.0000
NITROGEN	0.1986
OXYGEN	0.2975
CARBON MONOXIDE	0.2753
WATER	0.0002
HYDROGEN	0.2283
METHANE	0.0000
Errors	[none]

Figure 4.2. Syngas Reactor Final Product Composition

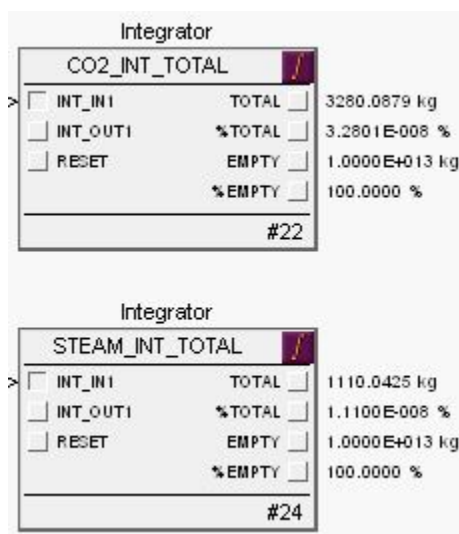


Figure 4.3. CO₂ and Steam quantity fed for the simulation

The Yield calculation for this real-time dynamic simulation model as:

3,280 kg of CO₂ & 1110 kg of Steam fed to the Syngas Reactor

CO₂ quantity = 3,280 kg = 74.54 kmol

Based on this quantity, Theoretical CO production = 74.54 kmol = 2088 kg and

H₂ produced = 124.18 kg.

Simulation Results after running for 3 hours, the final composition of Syngas reactor in the vapor mole fraction is shown in the Figure 4.2. The vapor Molar Holdup =

270.78 kmol, therefore, Actual vapor CO kmol = (0.2753*270.78 kmol) = 74.545 kmol

Reaction Conversion or Process Yield = (Actual mol % / Theoretical mol %) * 100

$$= (27.53 / 27.4) * 100 \approx 100 \%$$

In the Table 4.1, the theoretical and actual simulation results are shown for the production of Syngas based on the quantity of carbon dioxide produced from the aluminum smelting process.

Table 4.1. Theoretical and Actual (simulation) Results

Components	MW (kg/kmol)	Theoretical (kg)	Theoretical (kmol)	Theoretical Mole %	Simulation Mole % (liquid)	Reaction Conversion or Yield
Al	26.98	0	0	0	0	≈100%
C	12	0	0	0	0	
Al ₂ O ₃	101.96	0	0	0	0	
CO ₂	44	3280	74.54	27.4	6.64E-40	
NaF	41.99	0	0	0	0	
AlF ₃	83.98	0	0	0	0	
N ₂	28.01	0	0	0	0	
O ₂	32	0	0	0	0	
CO	28.01	2088	74.54	27.4	27.53	
H ₂ O	28.01	1110	61.6	22.6	0.02	
H ₂	32	124.18	61.6	22.6	22.83	
CH ₄	28.01	0	0	0	0	

5. CONCLUSION AND FUTURE WORK

A Dynamic Simulation Model of high temperature Co-electrolysis has been developed using Mimic Process Simulator software to utilize the carbon dioxide emitted from aluminum smelting process for the direct production of Syngas. The high temperature co-electrolysis of steam and carbon dioxide appears to be a promising technology that could provide a possible path to reduce greenhouse gases emissions and an attractive application to convert the Syngas further into synthetic liquid fuels through the Fischer Tropsch process.

The dynamic cell energy balance model is constructed using Mimic Software standard model with programming and then applied to this Syngas reactor. The results of this research work simulation successfully demonstrates the behavior of the solid oxide electrolytic cell and the control system, although further coarse tuning of mass and energy requirement parameters would be more realistic based on actual experimental or industrial operating production data.

The high temperature solid oxide electrolytic cell is identified as a most promising technology because of non-carbon emitting advanced nuclear energy, sustainable water splitting technology, energy efficient high temperature process, three processes develop in parallel and reaction kinetics of RWGSR are better at elevated temperature of electrolysis cell electrode. Even though the high temperature Co-electrolysis model developed provides a good representation of the physical system, there are many phenomena that were not taken into consideration. The further studies would be a direct continuation of the work described as

- The diffusion rate of O_2 through Ni cathode surface and YSZ (yttria stabilized zirconium electrolyte) interface in a Solid Oxide Electrolytic cell
- The modeling of the current distribution and the magnetic fields in the cell
- The modeling of possibilities of side reactions like Boudouard reaction and electrochemical reactions ionization effect of the compounds
- As an energy-intensive process, the major contributor to the production cost of Syngas is the electricity cost. Therefore, determining the detailed economic competitiveness of this process would play a decisive role to evaluate the economic feasibility.

REFERENCES

1. Fu Qinqxi, Mabilat C., Syngas production via high-temperature steam/CO₂ co-electrolysis: an economic assessment, European Institute of Energy Research, Energy & Environmental Science, Issue 10, July 2010.
2. Hawkes Grant, O'Brien James, Shoots Carl, Jones Russel, 3D CFD Model of High Temperature H₂O/CO₂ Co-electrolysis, ANS Summer Meeting, June 2007.
3. Shoots Carl, O'Brien James, Herring J., Hartvigen Joseph, Syngas Production via High-Temperature Coelectrolysis of Steam and Carbon Dioxide, Idaho National Laboratory, Journal of Fuel Cell Science and Technology, Volume 6, Nov 2008.
4. Shoots Carl, Production of Synthesis Gas by High-Temperature Electrolysis of H₂O and CO₂ (Coelectrolysis), Idaho National Laboratory, May 2010.
5. O'Brien J., Stoots C., Herring J., Hartvigsen J., High-Temperature Co-Electrolysis of Steam and Carbon Dioxide for Direct Production of Syngas; Equilibrium Model and Single-Cell Tests, Idaho National Laboratory, Fifth International Fuel Cell Science Engineering and Technology Conference, July 2007.
6. Shoots C., O'Brien J., Hartvigsen J., Carbon Neutral Production of Syngas via High Temperature Electrolytic Reduction of Steam and CO₂. Idaho National Laboratory, ASME 2007 International Mechanical Engineering Congress and Exposition, Nov 2007.
7. Hartvigsen J., Frost L., Elangovan S., High Temperature Co-Electrolysis of Steam and Carbon Dioxide Using Wind Power, Ceramatec Inc., Fuel Cell Seminar & Exposition Mohegan Sun, November 2012.
8. Chen Chen, Smith Joseph D., Process Modeling of High Temperature Electrolysis for Liquid Fuel Production, AIChE Annual Meeting Salt Lake City Utah, November 2010.
9. Ni Meng, An electrochemical model for Syngas production by co-electrolysis of H₂O and CO₂, Building Energy Research group. Journal of Power Sources, December 2011.

10. Wolf Andreas, Jess Andreas, Kern Christoph, Syngas Production via Reverse Water-Gas Shift Reaction over a Ni-Al₂O₃ Catalyst: Catalyst Stability, Reaction Kinetics, and Modeling. *Chemical Engineering & Technology*, Volume 39, Issue 6, February 2016.
11. Laguna-Bercero M. A., Skinner S. J., Kilner J. A., Performance of Solid Oxide Electrolysis Cells Based on Scandia Stabilized Zirconia, *Journal of Power Sources*, Volume 192, Issue 1, July 2009.
12. Graves Christopher, Ebbesen Sune, Mogensen Mogens, Lackner Klaus, Sustainable hydrocarbon fuels by recycling CO₂ and H₂O with renewable or nuclear energy, *Renewable and Sustainable Energy Reviews*, Volume 15, Issue 1, January 2011.
13. O'Brien J., Stoots C., Herring J., Hartvigsen J., Hydrogen Production performance of a 10-Cell Planar Solid-Oxide Electrolysis Stack, Idaho National Laboratory, ASME 2005 3rd International Conference on Fuel Cell Science, Engineering and Technology, May 2005.
14. Stempien Jan, Ni Meng, Sun Qiang, Hwa Siew, Thermodynamic analysis of combined Solid Oxide Electrolyzer and Fischer-Tropsch processes. *Energy (Oxford) journal*, Volume 47, Issue 8, March 2015.
15. Retrieved data and Statistics from:
<https://www.mynah.com/resources>
www.kinetics.nist.gov/janaf
<http://www.ceramatec.com>
www.calsmelt.com.
16. Chase, Malcolm W. Jr., et al. JANAF Thermochemical Tables, 3rd Edition, Washington DC: American Chemical Society, 1985.

SECTION

2. CONCLUSIONS

A Mimic Dynamic Simulation model with rigorous kinetics have been developed for an aluminum smelting process and high temperature Steam/CO₂ Co-electrolysis in an electrolytic reduction cell. This work demonstrates and predicts the dynamic behavior of the critical operation of aluminum smelter and evaluates strategies for alternative design or uses of a Nuclear Power Small Modular Reactor (SMR) to explore intensive process heat energy requirement and to improve process efficiency.

With the increasing energy demand, decrease of the availability of cheap electricity and the need to reduce greenhouse gases emission, this aluminum smelting production plant employs a high temperature Co-electrolysis unit for the utilization of carbon dioxide from the smelting process for the production of Synthetic gas. By coupling a nuclear power SMR with HTCE unit, the emitted carbon dioxide can be used to generate Syngas through steam electrolysis and reverse water gas shift reaction. This process offers most promising technology because of non-carbon emitting advanced nuclear energy, sustainable water splitting, energy efficient high temperature process and three parallel reactions occurs in a solid oxide electrolytic cell.

Future work can be to validate these dynamic process models with actual industrial data or experimental data for different operating facilities and perform a techno-economic analysis of both models. Future plan is to integrate diffusion rate of O₂ through Ni cathode and yttria stabilized zirconium electrolyte in a solid oxide electrolytic cell for the production of Syngas via high temperature Co-electrolysis.

APPENDIX

THERMOCHEMICAL PROPERTIES OF CHEMICAL COMPOUNDS

Table 1: The enthalpy of formation of various substances involved in the aluminum reduction process. Taken from JANAF [16]

Chemical Substance		ΔH_f° (kJ·mol ⁻¹)		
		T=1100°K	T=1200°K	T=1300°K
Aluminum (l)	Al	0	0	0
Aluminum Fluoride (s)	AlF ₃	-1509.431	-1507.984	-1506.471
Aluminum Oxide (α)	Al ₂ O ₃	-1692.437	-1691.366	-1690.190
Aluminum Oxide (γ)	Al ₂ O ₃	-1669.354	-1667.684	-1665.902
Carbon (s)	C	0	0	0
Carbon Monoxide (g)	CO	-112.586	-113.217	-113.870
Carbon Dioxide (g)	CO ₂	-394.838	-395.050	-395.257
Hydrogen (g)	H ₂	0	0	0
Hydrogen Fluoride (g)	HF	-274.896	-275.231	-275.558
Water (g)	H ₂ O	-248.460	-248.997	-249.473
Sodium Tetrafluoroaluminate (g)	NaAlF ₄	-1859.349	-1956.723	-1956.466
Cryolite (β,l)	Na ₃ AlF ₆	-3196.537	-3470.530	-3451.697
Sodium Carbonate (s)	Na ₂ CO ₃	-1110.305	-1297.547	-1289.016
Sodium Oxide (γ,β)	Na ₂ O	-412.418	-603.913	-588.116
Sodium Fluoride (s)	NaF	-572.322	-667.607	-448.581
Sulfur (s)	S	0	0	0
Sulfur Dioxide (g)	SO ₂	-361.835	-361.720	-361.601

Table 2: The Entropy of various substances involved in the aluminum reduction process. Taken from JANAF [16]

Chemical Substance		ΔS° (J·K ⁻¹ ·mol ⁻¹)		
		T=1100°K	T=1200°K	T=1300°K
Aluminum (l)	Al	76.426	79.189	81.730
Aluminum Fluoride (s)	AlF ₃	189.147	198.057	206.334
Aluminum Oxide (α)	Al ₂ O ₃	192.189	203.277	213.602
Aluminum Oxide (γ)	Al ₂ O ₃	200.178	211.787	222.597
Carbon (s)	C	26.548	28.506	30.346
Carbon Monoxide (g)	CO	237.726	240.679	243.431
Carbon Dioxide (g)	CO ₂	274.528	279.390	283.932
Hydrogen (g)	H ₂	169.112	171.790	174.288
Hydrogen Fluoride (g)	HF	212.168	214.845	217.340
Water (g)	H ₂ O	236.731	240.485	244.035
Sodium Tetrafluoroaluminate (g)	NaAlF ₄	502.077	513.392	523.836
Cryolite (β,l)	Na ₃ AlF ₆	659.829	694.243	725.901
Sodium Carbonate (s)	Na ₂ CO ₃	334.537	377.525	392.696
Sodium Oxide (γ,β)	Na ₂ O	186.205	194.645	212.098
Sodium Fluoride (s)	NaF	120.289	125.768	157.380
Sulfur (s)	S	137.187	138.829	140.352
Sulfur Dioxide (g)	SO ₂	310.995	315.824	320.310

VITA

Rajesh Patharabe was born on October 7, 1986 in Nagpur, India. Rajesh earned his Bachelor's degree in Chemical Engineering from top ranked Laxminarayan Institute of Technology, Nagpur, India in May 2008. In his senior year, he worked on his dissertation project on "Supercritical fluid extraction technique and its application in chemical industries" under Professor Dr. Srikanth Dawande.

After his B.S. in Chemical Engineering in Spring 2008, he joined United Phosphorus Limited organization as a process engineer and worked there in Tri-methyl Phosphite and Ammonium Chloride plant for three and half years. In addition, he also worked at Thermax Limited and B. Y. Agro & Infra Pvt. Ltd. for almost one year.

In Spring 2014, he began his Master of Science program in Chemical Engineering at Missouri University of Science and Technology, Rolla. He worked at MYNAH Technologies as a Simulation Project Co-op Engineer from Spring 2015 till the end of Fall 2015. During the 2016 academic year, he joined Dr. Joseph Smith's Laufer Energy research group and worked as a graduate research assistant. Rajesh graduated with his Master of Science in Chemical Engineering in May, 2017.